Dynamic Games and Applications (2020) 10:257–296
https://doi.org/10.1007/s13235-019-00307-1

A Dynamic Game Approach to Uninvadable Strategies for Biotrophic Pathogens

Ivan Yegorov[1] · Frédéric Grognard[2] · Ludovic Mailleret[2,3] · Fabien Halkett[4] · Pierre Bernhard[2]

Published online: 28 March 2019

Abstract
This paper studies a zero-sum state-feedback game for a system of nonlinear ordinary differential equations describing one-seasonal dynamics of two biotrophic fungal cohorts within a common host plant. From the perspective of adaptive dynamics, the cohorts can be interpreted as resident and mutant populations. The invasion functional takes the form of the difference between the two marginal fitness criteria and represents the cost in the definition of the value of the differential game. The presence of a specific competition term in both equations and marginal fitnesses substantially complicates the reduction in the game to a two-step problem that can be solved by using optimal control theory. Therefore, a general game-theoretic formulation involving uninvadable strategies has to be considered. First, the related Cauchy problem for the Hamilton–Jacobi–Isaacs equation is investigated analytically by the method of characteristics. A number of important properties are rigorously derived. However, the complete theoretical analysis still remains an open challenging problem due to the high complexity of the differential game. That is why an ad hoc conjecture is additionally proposed. An informal but rather convincing and practical justification for the latter relies on numerical simulation results. We also establish some asymptotic properties and provide biological interpretations.

Keywords Uninvadable strategy · Zero-sum differential game · Biotrophic pathogens · Resource allocation · State-feedback control · Hamilton–Jacobi–Isaacs equation · Method of characteristics · Finite-difference approximation

Ivan Yegorov: Also known as I. Egorov.

Electronic supplementary material The online version of this article (https://doi.org/10.1007/s13235-019-00307-1) contains supplementary material, which is available to authorized users.

✉ Ivan Yegorov
ivanyegorov@gmail.com

1 North Dakota State University, Fargo, USA

2 Inria, INRA, CNRS, Sorbonne Université, Biocore Team, Université Côte d'Azur, Nice, France

3 INRA, CNRS, ISA, Université Côte d'Azur, Nice, France

4 UMR IAM, INRA, Université de Lorraine, Nancy, France

1 Introduction

In compliance with Darwin's Theory of Evolution by Natural Selection, it is relevant to model the mechanisms by which various biological species allocate available resources with the objective either to maximize their fitness criteria or to prevent invasions of others [55]. The first type of strategies is usually governed by specific optimality principles for relatively isolated homogeneous populations and hence may not be reasonable in case of competition for common resources between different populations or between resident and mutant genotypes. For instance, the mutants may take evolutionary advantage by acting differently from the residents.

A number of mathematical techniques have been developed to study the strategies that can be selected through evolution among competing genotypes. Adaptive dynamics is of particular interest there. This methodology is based upon the analysis of how resident populations allow or prevent invasions by rare mutants [19,25]. The concept of evolutionary stable strategy (or, in short, ESS) originally introduced in the context of evolutionary game theory [32,33] plays a crucial role in adaptive dynamics. An ESS can informally be described as a point in the trait space at which no mutant population can invade. ESS-es therefore lead to evolutionary equilibria [19, Sect. 3.7]. Despite their name, ESS-es may nevertheless form (dynamically) unstable equilibria [22,38].

Classical results of adaptive dynamics focused mainly on finite-dimensional traits. However, many actual dynamic life-history characteristics could have an infinite-dimensional nature, especially those subjected to dilemmas of resource allocation. Therefore, some recent developments in adaptive dynamics considered function-valued traits [9,10,20,36,41]. The following approach to computing ESS-es was proposed in [10,36]: maximize the invasion fitness over admissible mutant strategies u_{mut} and thereby construct the set of maximizers $U^*_{\mathrm{mut}}(u_{\mathrm{res}})$ depending on an admissible resident strategy u_{res}; then a solution $\hat{u}_{\mathrm{res}}$ to the inclusion $u_{\mathrm{res}} \in U^*_{\mathrm{mut}}(u_{\mathrm{res}})$ is an ESS if the corresponding invasion fitness maximizer is unique, i. e., if $U^*_{\mathrm{mut}}(\hat{u}_{\mathrm{res}}) = \{\hat{u}_{\mathrm{res}}\}$. The latter uniqueness ensures that the related symmetric Nash equilibrium is strict and consequently represents an ESS (see [50, Sect. 2.1]). But efficient practical applications of this approach (including the usage of Pontryagin's maximum principle from optimal control theory [42]) were limited to models in which the resident dynamics and fitness did not explicitly depend on the mutant population. Otherwise, one has to use the general formulation of [10, Sect. 4.1] involving the concepts of uninvadable strategy and Wardrop equilibrium and leading to a zero-sum two-player differential game.

The aim of this work is to investigate a game-theoretic extension of the dynamic optimization problem of [56]. The latter was to find a resource allocation strategy maximizing the pathogen fitness (analogous to the lifetime reproductive success) for one-seasonal development of a single biotrophic fungal cohort within one host plant.

Biotrophic fungi are an important group of plant pathogens [18,27]. The mass of branching and thread-like hyphae constituting the vegetative part of such a fungus is called the mycelium. The fungi permeate living host plant cells and obtain nutrients from the latter via specific absorbing organs that appear as outgrowths of the somatic hyphae and are called haustoria. Thereby, the hosts are harmed but not killed. In natural environments, this kind of parasitism decreases competitive abilities of plants. It also reduces yields in agricultural systems. A significant subclass of biotrophic fungi contains rust fungi causing such diseases as leaf rusts of poplar, willow, wheat, blackberry, etc. Another subclass consists of powdery mildew fungi infecting such emblematic/cultivated species as oaks, grapes, hawthorn, gooseberry, etc., and, of course, many species of wild plants. The model of [56] considered a biotrophic

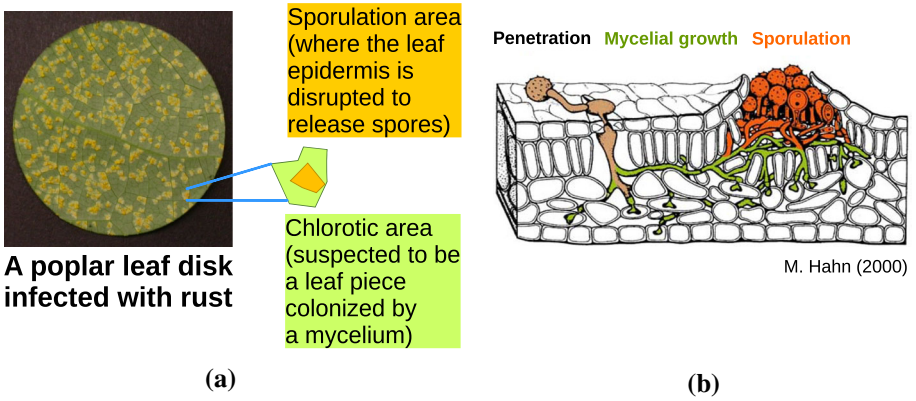

Fig. 1 (**a**) Rust lesions scattered on a poplar leaf disk in a laboratory experiment. When zooming in on a lesion, one can distinguish an orange-yellow sporulation area (corresponding to the spores produced by the lesion) and a pale yellow-green chlorotic area (colonized by a mycelium). Note that chlorotic areas are not always clearly visible, depending on host genetic backgrounds. (**b**) Schematic illustration of a rust infection cycle, as presented in [27]. The permission to use this illustration in the current paper was obtained from Springer Nature via an order through Copyright Clearance Center's RightsLink® service (the license number 4513210982653) (Color figure online)

fungal cohort allocating available host resources between two different activities, namely mycelial growth (within-host multiplication) and sporulation (production of spores for outer transmission of the infection). Some related illustrations are given in Fig. 1.

In [56], the constructed feedback form of the optimal allocation strategy indicated a key role of a singular regime with coexisting activities (after the onset of sporulation). This is common among biotrophic fungi (see, e.g., [3,13,51], and note that, if the average mycelium size remains nearly constant during sporulation, some resources should still be allocated to mycelial growth in order to compensate mycelial decay), contrary to saprophytic fungi (obtaining nutrients from dead organic matter), for which optimal allocation strategies are purely bang–bang according to the results of [26]. Game-theoretic extensions of such dynamic models are worth investigating, since they can help to describe possible evolutionary equilibria in the realistic situations where several pathogen cohorts (with different genotypes) compete with each other for common resources within one host.

For simplicity, we study one-seasonal dynamics of only two biotrophic fungal cohorts within one host plant and assume constant lesion densities. From the perspective of adaptive dynamics, they can be interpreted as resident and mutant cohorts. The single-state dynamic equation and corresponding optimization criterion in [56] are now replaced with two-state dynamic equations and a suitable invasion functional (in the form of the difference between the two marginal fitness criteria). In both equations and both marginal fitnesses, there appears a so-called competition term that depends on both state variables if the lesion densities do not vanish. It is not clear what reasonable ways can be proposed in order to neglect the direct dependence of the resident dynamic equation and marginal fitness on the mutant state variable by assuming that the mutant lesion density is small in comparison with the resident one. Furthermore, competition between two pathogen cohorts with comparable lesion densities can be of interest by itself. These circumstances substantially complicate the use of the aforementioned two-step approach of [10,36,41] relying on optimal control theory. Hence, we have to consider a zero-sum two-player differential game by employing the formulation of [10, Sect. 4.1]. Also note that, compared to optimal control problems, investigation of

differential games turns out to be essentially more difficult [5–8,30,34,52,57]. (A detailed mathematical discussion in connection with our problem is given in Sect. 2.)

Bearing in mind the general discussions in [1,10], we do not have clear evidence of mutual cooperation between the resident and mutant populations. Those works point out that, in case when residents treat mutants as cooperators and keep using a collective optimal control strategy, the mutants refusing to cooperate in such a way may invade and eventually outcompete the residents. It is therefore reasonable to consider uninvadable and evolutionary stable strategies.

The paper is organized as follows. Section 2 provides a detailed statement of the problem. In Sect. 3, we analytically investigate the zero-sum two-cohort differential game. A number of important properties are rigorously derived. However, the complete theoretical analysis still remains an open challenging problem due to the high complexity of the differential game. That is why an ad hoc conjecture has to be additionally proposed. An informal but rather convincing and practical justification for the latter is given in Sect. 4 and based on numerical simulation results. Section 5 presents some asymptotic properties. In Sect. 6, we summarize the obtained analytical and numerical results together with their biological interpretations. The paper is also supported by electronic supplementary material consisting of two appendices. In Online Appendix A, we recall the central results of the previous work [56] regarding the optimal control problem for a single cohort. Compared to [56], slightly refined formulations and some new properties are provided. This helps to better understand similar reasoning in Sect. 3.3.1. Online Appendix B accompanies the investigation in Sects. 3.2 and 3.3.2.2.

2 Problem Statement

2.1 Dynamic Model

Consider one-seasonal dynamics of two biotrophic fungal cohorts within one host plant. Let us refer to them as to cohorts 1 and 2. For cohort i, denote the lesion density, i.e., the number of mycelia per unit area of the host, by n_i. For simplicity, we assume that n_1, n_2 are constant during the whole infection period within the season. This means that new infectious agents do not penetrate into the host during the observed period, i.e., only the already present infections develop. Although this is in general a strong restriction for infections *in natura*, it still allows to obtain important results with relevant biological interpretations (as will be shown in the current work) and is reasonable in particular for experimental infection protocols (when, e. g., a suspension of spores is sprayed on a leaf surface at a given date, and all related mycelia further develop in laboratory conditions and have almost the same age). Denote the average size of a mycelium in cohort i by M_i. Let S_i be the average quantity of spores produced by a mycelium in cohort i. The infection age t within the season is interpreted as a time variable.

The nutrient flux uptaken by cohort i is specified by a function $f_i = f_i(M_1, M_2)$ and allocated between two different pathogen activities such as within-host multiplication (mycelial growth) and production of asexual spores. Let $u_i = u_i(t)$ be a related resource allocation function taking values between zero and one. Adopt that the whole flux goes to mycelial growth when $u_i(t) = 0$ and to spore production when $u_i(t) = 1$, while, for $0 < u_i(t) < 1$, there is an intermediate configuration. A similar approach to representing resource allocation functions was used in the model of [26] describing life-history strategies of saprophytic fungi, as well as in the general consumer–resource models studied in [1,2,10].

For both cohorts, let the rate of mycelial decay be determined by a function $g = g(M)$. Also suppose that, compared to mycelial growth, spores are produced with a constant yield $\delta > 0$.

The time span of the infections within the season is the interval $[0, T]$. The time horizon $T > 0$ is fixed and can be finite or infinite. The infinite-horizon case is a reasonable abstraction when the pathogen dynamics is rather fast with respect to the whole infection duration. If $T = +\infty$, we understand $[0, T]$ as $[0, +\infty)$.

Thus, we arrive at the following dynamic model:

$$\begin{cases} \dfrac{\mathrm{d}M_1(t)}{\mathrm{d}t} = (1 - u_1(t))\, f_1(M_1(t), M_2(t)) - g(M_1(t)), \\ \dfrac{\mathrm{d}M_2(t)}{\mathrm{d}t} = (1 - u_2(t))\, f_2(M_1(t), M_2(t)) - g(M_2(t)), \\ \dfrac{\mathrm{d}S_1(t)}{\mathrm{d}t} = \delta\, u_1(t)\, f_1(M_1(t), M_2(t)), \\ \dfrac{\mathrm{d}S_2(t)}{\mathrm{d}t} = \delta\, u_2(t)\, f_2(M_1(t), M_2(t)), \\ M_1(0) = M_1^0, \quad M_2(0) = M_2^0, \quad S_1(0) = S_1^0, \quad S_2(0) = S_2^0, \\ 0 \leqslant u_1(t) \leqslant 1, \quad 0 \leqslant u_2(t) \leqslant 1, \quad t \in [0, T]. \end{cases} \tag{1}$$

For brevity, we do not explicitly show dependence on the constant parameters n_1, n_2 when writing $f_i = f_i(M_1, M_2)$, $i = 1, 2$.

Since the right-hand sides of all four dynamic equations in (1) do not contain S_1, S_2, we do not need to treat S_1, S_2 explicitly, i.e., M_1, M_2 can be considered as the only state variables.

As in [56, Section 7], the mycelial sizes M_1, M_2 can be measured in terms of equivalent amounts of infecting spores. In particular, if a mycelium appears from one spore at the beginning of the infection period, the initial mycelial size can be set as one equivalent of an infecting spore or, simply, as one spore. If one also measures time (infection age) in days and area of the host in cm^2, then the lesion densities n_1, n_2 are measured in $\mathrm{spores/cm}^2$, the nutrient fluxes f_1, f_2 and the decay rate g are measured in $\mathrm{spores/day}$, while the control variables u_1, u_2 and the yield parameter δ are dimensionless.

First, let us formulate the hypotheses that will be used all along the paper.

Assumption 2.1 The following holds:

(1) $f_i = f_i(M_1, M_2)$, $i = 1, 2$, are twice continuously differentiable functions defined for all $M_1 \geqslant 0$, $M_2 \geqslant 0$ and taking nonnegative values;
(2) for $i = 1, 2$, we have $f_i(M_1, M_2) = 0$ if $M_i = 0$, and $f_i(M_1, M_2) > 0$ if $M_i > 0$;
(3) $g = g(M)$ is a twice continuously differentiable function defined for all $M \geqslant 0$;
(4) $g(0) = 0$, and $g(M) > 0$ for $M > 0$;
(5) there exist sufficiently large numbers $\bar{M}_1 > 0$, $\bar{M}_2 > 0$ such that

$$f_1\left(\bar{M}_1, M_2\right) - g\left(\bar{M}_1\right) < 0 \quad \forall M_2 \in \left[0, \bar{M}_2\right],$$
$$f_2\left(M_1, \bar{M}_2\right) - g\left(\bar{M}_2\right) < 0 \quad \forall M_1 \in \left[0, \bar{M}_1\right].$$

Assumption 2.1 implies that, for any initial coordinates $M_i^0 \in \left(0, \bar{M}_i\right)$, $i = 1, 2$, and for any Lebesgue measurable functions $u_i : [0, T] \to [0, 1]$, $i = 1, 2$, the system of the first two equations in (1) admits a unique trajectory $[0, T] \ni t \longmapsto (M_1(t), M_2(t)) \in \mathbb{R}^2$, and

$$M_i(t) \in \left(0, \bar{M}_i\right) \quad \forall t \in [0, T], \quad i = 1, 2.$$

Hence, the domain

$$G \stackrel{\text{def}}{=} \left\{(M_1, M_2) \in \mathbb{R}^2 : 0 < M_1 < \bar{M}_1,\ 0 < M_2 < \bar{M}_2\right\} \tag{2}$$

is a bounded strongly invariant set in the state space for our controlled system [14, Chapter 4, Sect. 3].

The constants $\bar{M}_1, \bar{M}_2$ can be interpreted as carrying capacity estimates.

Let us consider only the state trajectories that lie in the strongly invariant domain (2).

Assumption 2.2 $(M_1^0, M_2^0) \in G$.

In the single-cohort case, when one pathogen cohort is absent, the fitness criterion for remaining cohort i is specified as maximization of the lifetime reproductive success, which is a common definition of fitness in Ecology and Evolutionary Studies [35], and which can here be reduced to the expected reproductive output [16,17,46]. In line with [26,56], the latter is characterized by $\int_0^T (\mathrm{d}S_i(t)/\mathrm{d}t)\, e^{-\mu t}\, \mathrm{d}t$, where $\mathrm{d}S_i(t)/\mathrm{d}t$ is the spore production rate at the infection age t (this rate in particular depends on the corresponding mycelial size $M_i(t)$), and $e^{-\mu t}$ is a term describing exponential extinction of the infections with a constant parameter $\mu > 0$ (the probability density function of the related exponential distribution is determined as $\mu\, e^{-\mu t}$ for all $t \geqslant 0$, and omitting the constant positive factor μ leads to an equivalent criterion). In the double-cohort case governed by system (1), this criterion is affected by both cohorts and can informally be written as

$$J_i(u_1(\cdot), u_2(\cdot)) \stackrel{\text{def}}{=} \int_0^T u_i(t)\, f_i(M_1(t), M_2(t))\, e^{-\mu t}\, \mathrm{d}t \longrightarrow \sup_{u_i(\cdot)}$$

(since δ is a positive constant).

The next assumption represents some biological aspects of the model in more detail.

Assumption 2.3 The nutrient fluxes are determined by

$$f_i(M_1, M_2) \stackrel{\text{def}}{=} \nu(n_1 M_1 + n_2 M_2) \cdot \rho(M_i) \quad \forall M_1 \geqslant 0 \quad \forall M_2 \geqslant 0, \quad i = 1, 2, \tag{3}$$

where the function $\rho\colon [0, +\infty) \to [0, +\infty)$ specifies the resource flows that can be obtained by a single mycelium and the function $\nu\colon [0, +\infty) \to (0, +\infty)$ describes the negative influence of competition between mycelia for host resources. Moreover, $\rho(\cdot)$, $\nu(\cdot)$ are twice continuously differentiable on $[0, +\infty)$, $\rho(0) = 0$, and $\rho(M) > 0$ for $M > 0$.

The functions (3) satisfy $f_1(M, M) = f_2(M, M)$ for all $M \geqslant 0$, which yields the property that $J_1(u_1(\cdot), u_2(\cdot)) = J_2(u_1(\cdot), u_2(\cdot))$ if $M_1^0 = M_2^0$ and Lebesgue measurable functions $u_i\colon [0, T] \to [0, 1]$, $i = 1, 2$, are equivalent (i.e., equal to each other almost everywhere on the time interval $[0, T]$ with respect to Lebesgue measure).

Depending on the sections below, the following properties of the functions $\nu(\cdot)$, $\rho(\cdot)$, $g(\cdot)$ will also be imposed.

Assumption 2.4 Denote

$$\bar{M}_{\min} \stackrel{\text{def}}{=} \min\left(\bar{M}_1, \bar{M}_2\right), \quad \bar{M}_{\max} \stackrel{\text{def}}{=} \max\left(\bar{M}_1, \bar{M}_2\right),$$
$$n \stackrel{\text{def}}{=} n_1 + n_2.$$

The following conditions hold:

(1) $\nu'(x) \leqslant 0$ for $x \in \left[0, n_1\bar{M}_1 + n_2\bar{M}_2\right]$;
(2) $\rho'(M) \geqslant 0$ and $\rho''(M) \leqslant 0$ for $M \in \left[0, \bar{M}_{\max}\right]$;
(3) $g'(M) \geqslant 0$ and $g''(M) \geqslant 0$ for $M \in \left[0, \bar{M}_{\max}\right]$;
(4) either $\nu'(\cdot), \rho'(\cdot)$ are nonzero everywhere on $\left(0, n_1\bar{M}_1 + n_2\bar{M}_2\right)$ and $\left(0, \bar{M}_{\max}\right)$, respectively, or $\rho''(\cdot)$ is nonzero everywhere on $\left(0, \bar{M}_{\max}\right)$;
(5) in the degenerate case $n = 0$, we adopt that $\rho''(M) < 0$ for $M \in \left(0, \bar{M}_{\max}\right)$;
(6) $\nu(0) \cdot \rho'(0) - g'(0) > \mu$;
(7) there exists $\tilde{M} \in \left(0, \bar{M}_{\min}\right)$ such that

$$\nu\left(n\tilde{M}\right) \cdot \rho'\left(\tilde{M}\right) - g'\left(\tilde{M}\right) < \mu.$$

Assumption 2.5 In items 1–3 of Assumption 2.4, the intervals are extended up to $+\infty$, its items 4,5 are replaced merely with negativity of $\rho''(\cdot)$ on $(0, +\infty)$ regardless of n, and in its item 7, $\tilde{M} \in \left(0, \bar{M}_{\min}\right)$ is replaced with $\tilde{M} > 0$.

Assumption 2.6 $\lim\limits_{x \to +\infty} \nu(x) = 0$, and $\rho'(\cdot)$ is bounded on $[0, +\infty)$.

Remark 2.7 In particular, items 1–3 of Assumption 2.4 imply the following:

- $\nu(\cdot)$ is nonincreasing on $\left[0, n_1\bar{M}_1 + n_2\bar{M}_2\right]$ (which is reasonable for the competition term with a growth reduction property);
- $\rho(\cdot)$ is nondecreasing and concave on $\left[0, \bar{M}_{\max}\right]$. (a typical example is the classical Michaelis–Menten law [37] with a saturating growth behavior, as given in Example 2.8);
- $g(\cdot)$ is nondecreasing and convex on $\left[0, \bar{M}_{\max}\right]$ (which holds for the linear decay rate given in Example 2.8).

Furthermore, items 4–7 of Assumption 2.4 will also be required in Sect. 3.1, and Assumptions 2.5, 2.6 will be used in Sect. 5. □

Other assumptions will be formulated when needed in the subsequent sections.
Besides, we will also use Dieudonné's notation:

$$\begin{aligned} &\mathrm{D}_i f_j \stackrel{\text{def}}{=} \frac{\partial f_j}{\partial M_i}, \quad \mathrm{D}_i[f_j - f_l] \stackrel{\text{def}}{=} \frac{\partial (f_j - f_l)}{\partial M_i}, \\ &\mathrm{D}_{ij} f_l \stackrel{\text{def}}{=} \frac{\partial^2 f_l}{\partial M_i \partial M_j}, \quad \mathrm{D}_{ij}[f_l - f_q] \stackrel{\text{def}}{=} \frac{\partial^2 (f_l - f_q)}{\partial M_i \partial M_j}, \\ &i = \overline{1,2}, \quad j = \overline{1,2}, \quad l = \overline{1,2}, \quad q = \overline{1,2}. \end{aligned} \tag{4}$$

Example 2.8 Introduce positive constants α, k, β, γ and let

$$\rho(M) = \alpha \frac{M}{M + k} \quad \forall M \geqslant 0, \tag{5}$$

$$\nu(n_1 M_1 + n_2 M_2) = \frac{1}{1 + \beta\,(n_1 M_1 + n_2 M_2)} \quad \forall M_1 \geqslant 0 \quad \forall M_2 \geqslant 0, \tag{6}$$

$$g(M) = \gamma M \quad \forall M \geqslant 0. \tag{7}$$

Let

$$\alpha > k\,(\gamma + \mu). \tag{8}$$

Then $\hat{M} \stackrel{\text{def}}{=} \alpha/\gamma - k$ is a unique positive root of the equation

$$\rho\left(\hat{M}\right) - g\left(\hat{M}\right) = \hat{M}\left(\frac{\alpha}{\hat{M} + k} - \gamma\right) = 0,$$

and, by taking $\bar{M}_1 = \bar{M}_2 > \hat{M}$, we satisfy item 5 of Assumption 2.1, while its other items and Assumption 2.3 trivially hold. Assumptions 2.4–2.6 can also be verified easily. In particular, item 6 of Assumption 2.4 follows directly from (8), and, in order to satisfy the inequality in its item 7, one can choose $\tilde{M} = \hat{M}$, since

$$\begin{aligned} \nu\left(n\hat{M}\right)\rho'\left(\hat{M}\right) - g'\left(\hat{M}\right) &= \frac{1}{1+\beta n\hat{M}}\,\alpha\,\frac{k}{\left(\hat{M}+k\right)^2} - \gamma \\ &\leqslant \alpha\,\frac{k}{\left(\hat{M}+k\right)^2} - \gamma = \frac{k\gamma^2}{\alpha} - \gamma < \gamma - \gamma = 0. \end{aligned}$$

□

Example 2.9 Let α, β, γ be positive constants. Consider the functions (6),(7) and also the linear function

$$\rho(M) = \alpha M \quad \forall M \geqslant 0$$

instead of (5). Then the nutrient fluxes (3) take the form

$$f_i(M_1, M_2) \stackrel{\text{def}}{=} \frac{\alpha M_i}{1+\beta\left(n_1 M_1 + n_2 M_2\right)} \quad \forall M_1 \geqslant 0 \quad \forall M_2 \geqslant 0. \tag{9}$$

Suppose that $n_1 > 0$, $n_2 > 0$, and $\alpha > \gamma + \mu$. It is not difficult to verify Assumptions 2.1, 2.3, 2.4, 2.6, but the condition that $\rho''(M) < 0$ for all $M > 0$ as imposed in Assumption 2.5 does not hold. Even though the nutrient fluxes (9) may seem to be more reasonable than those in Example 2.8, this is in fact not the case, as will be shown in Remark 5.2. □

Remark 2.10 For simplicity, the nutrient concentration does not explicitly appear as one more variable in our model. However, the limitation of nutrient resources can be taken into account by imposing appropriate conditions on the functions $\nu(\cdot)$, $\rho(\cdot)$, $g(\cdot)$ (see Remark 2.7 and Example 2.8). In particular, some biologically relevant asymptotic properties will be obtained in Sect. 5.

A separate differential equation for the nutrient concentration variable was incorporated in the model of [43] describing life-history evolution of biotrophic wheat fungal pathogens. The sensitivity of the latent infection period and certain fitness measures with respect to a number of parameters (in other words, with respect to different fertilization scenarios) was numerically studied. However, the consideration was restricted to bang–bang resource allocation strategies, while singular regimes with coexisting spore production and maintenance of mycelia could be reasonable for many types of biotrophic fungal pathogens, as we already mentioned in Introduction. Furthermore, competition between two or more pathogen cohorts using different resource allocation strategies was not studied in [43]. Developing novel consumer–resource-type models that combine some aspects of the models in [43] and in the current work is therefore a relevant subject of future research. □

For convenience, Table 1 lists the introduced variables, constant parameters, and functions constituting the fluxes in our dynamic model together with the corresponding measurement units. The parameters in the representations (5)–(7) are included as well.

Table 1 The variables, constant parameters, and functions constituting the fluxes in the proposed dynamic model together with the corresponding measurement units

Variables/functions/parameters	Description	Measurement units
t	Infection age (time variable)	Days
M_1, M_2	Average mycelium sizes in cohorts 1,2 (state variables)	Spore equivalents or, simply, spores (this convention is used hereafter)
S_1, S_2	Average quantities of spores produced per mycelium in cohorts 1,2	Spores
u_1, u_2	Resource allocation fractions for cohorts 1,2 (control variables)	Dimensionless
n_1, n_2	Lesion densities for cohorts 1,2	spores/cm^2
$f_1(M_1, M_2)$, $f_2(M_1, M_2)$	Nutrient fluxes for cohorts 1,2	Spores/day
$g(M_1)$, $g(M_2)$	Mycelial decay rates for cohorts 1,2	Spores/day
$v(n_1M_1 + n_2M_2)$	Competition term in the nutrient fluxes	Dimensionless
$\rho(M_1)$, $\rho(M_2)$	Specific resource flow terms in the nutrient fluxes	Spores/day
T	Time horizon	Days
δ	Sporulation yield parameter	Dimensionless
μ	Parameter in the dimensionless term $e^{-\mu t}$ describing exponential extinction of the infections	Day^{-1}
α	Rate constant in the particular representation (5) of $\rho(\cdot)$	Spores/day
k	Half-saturation constant in the particular representation (5) of $\rho(\cdot)$	Spores
β	Scaling parameter in the particular representation (6) of $v(\cdot)$	cm^2/spores^2
γ	Decay rate parameter in the linear representation (7) of $g(\cdot)$	Day^{-1}

For obtaining the numerical simulation results presented in the subsequent sections and in Online Appendix A, the representations (5)–(7) and the following parameter values were used:

$$\begin{aligned} &\alpha = 0.2 \cdot 10^4 \text{ spores/day}, \quad k = (1/6) \cdot 10^4 \text{ spores}, \\ &\beta = 10^{-5} \text{ cm}^2/\text{spores}^2, \quad \gamma = 0.06 \text{ day}^{-1}, \quad \mu = 0.03 \text{ day}^{-1}, \\ &n_1 = 9 \text{ spores/cm}^2, \quad n_2 = 1 \text{ spore/cm}^2, \quad n = 10 \text{ spores/cm}^2. \end{aligned} \tag{10}$$

Some comments on the selected parameter values can be found in [56, Section 7]. Note in particular that the values of α, k, γ, μ in (10) satisfy the inequality (8).

For brevity, the indicated measurement units will henceforth be omitted in the paper. (One will be able to easily retrieve them with the help of Table 1.)

2.2 Zero-Sum Two-Cohort Differential Game and Uninvadable Strategies

The work [56] investigated the single-cohort optimal control problem

$$\begin{cases} \dfrac{\mathrm{d}M(t)}{\mathrm{d}t} = (1-u(t))\, f(M(t)) - g(M(t)), \quad M(0) = M_0, \\ 0 \leqslant u(t) \leqslant 1, \quad t \in [0,T], \end{cases} \tag{11}$$

$$\int_0^T u(t)\, f(M(t))\, e^{-\mu t}\, \mathrm{d}t \quad \longrightarrow \quad \max, \tag{12}$$

where

$$f(M) \stackrel{\text{def}}{=} \nu(nM)\, \rho(M) \quad \forall M \geqslant 0, \quad n = \text{const} \geqslant 0$$

(see Online Appendix A including slightly refined formulations and some new properties).

In case of two pathogen cohorts, we employ the general theoretical framework of [10, Sect. 4.1] and study one-seasonal competition between the cohorts in terms of their average reproductive outputs by seeking the saddle control strategies of a suitable class in the following zero-sum two-player differential game:

$$\begin{cases} \dfrac{\mathrm{d}M_1(t)}{\mathrm{d}t} = (1-u_1(t))\, f_1(M_1(t), M_2(t)) - g(M_1(t)), \\ \dfrac{\mathrm{d}M_2(t)}{\mathrm{d}t} = (1-u_2(t))\, f_2(M_1(t), M_2(t)) - g(M_2(t)), \\ M_1(0) = M_1^0, \quad M_2(0) = M_2^0, \\ 0 \leqslant u_1(t) \leqslant 1, \quad 0 \leqslant u_2(t) \leqslant 1, \quad t \in [0,T], \end{cases} \tag{13}$$

$$J(u_1(\cdot), u_2(\cdot)) \quad \longrightarrow \quad \inf_{u_1(\cdot)} \sup_{u_2(\cdot)} \text{ or } \sup_{u_2(\cdot)} \inf_{u_1(\cdot)}, \tag{14}$$

$$\begin{aligned} J(u_1(\cdot), u_2(\cdot)) &\stackrel{\text{def}}{=} J_2(u_1(\cdot), u_2(\cdot)) - J_1(u_1(\cdot), u_2(\cdot)) \\ &= \int_0^T (u_2(t)\, f_2(M_1(t), M_2(t)) - u_1(t)\, f_1(M_1(t), M_2(t)))\, e^{-\mu t}\, \mathrm{d}t. \end{aligned} \tag{15}$$

For zero-sum two-player differential games, various concepts of lower and upper value functions, saddle points, and Nash equilibrium are called forth by various classes of control strategies, such as:

(1) open-loop strategies [24,29,40,47–49,57];
(2) Varaiya–Roxin–Elliott–Kalton (VREK) or, simply, nonanticipative strategies [21,23, 45,54,57];
(3) state-feedback or, more precisely, nonstationary state-feedback strategies [4–8,30,34, 52].

Let us explain the approach of [10, Sect. 4.1] to define uninvadable and evolutionary stable strategies and how it relates to our differential game statement.

From the perspective of adaptive dynamics, let us interpret cohort 1 as a resident and cohort 2 as a mutant. Denote the corresponding classes of considered strategies as $\mathcal{U}_1$ and

$\mathcal{U}_2$. For a pair of strategies $(u_1, u_2) \in \mathcal{U}_1 \times \mathcal{U}_2$, we agree that the resident is not invaded by the mutant if and only if

$$J(u_1, u_2) \stackrel{\text{def}}{=} J_2(u_1, u_2) - J_1(u_1, u_2) \leqslant 0.$$

A strategy $\hat{u}_1 \in \mathcal{U}_1$ is therefore uninvadable if and only if

$$J\left(\hat{u}_1, u_2\right) \leqslant 0 \quad \forall u_2 \in \mathcal{U}_2,$$

which is equivalent to

$$\sup_{u_2 \in \mathcal{U}_2} J\left(\hat{u}_1, u_2\right) \leqslant 0.$$

Such a $\hat{u}_1$ exists if

$$\inf_{u_1 \in \mathcal{U}_1} \sup_{u_2 \in \mathcal{U}_2} J(u_1, u_2) = \min_{u_1 \in \mathcal{U}_1} \sup_{u_2 \in \mathcal{U}_2} J(u_1, u_2) \leqslant 0 \tag{16}$$

or

$$\inf_{u_1 \in \mathcal{U}_1} \sup_{u_2 \in \mathcal{U}_2} J(u_1, u_2) < 0 \tag{17}$$

(the latter inequality is mentioned in order to include the case when the infimum with respect to u_1 is not reached). This motivates the game-theoretic statement (13)–(15), where the first player tries to maximize its resistance to an invasion by the second one, and vice versa. If $M_1^0 = M_2^0$ and $\mathcal{U}_1 = \mathcal{U}_2 = \mathcal{U}$, then $J(u, u) = 0$ for all $u \in \mathcal{U}$, (17) cannot hold, and (16) is simplified to the equality

$$\min_{u_1 \in \mathcal{U}} \sup_{u_2 \in \mathcal{U}} J(u_1, u_2) = 0.$$

In this case, a strategy

$$\hat{u}_1 \in \operatorname{Arg} \min_{u_1 \in \mathcal{U}} \left(\sup_{u_2 \in \mathcal{U}} J(u_1, u_2) \right)$$

is an ESS if the related maximum with respect to u_2 is unique:

$$\operatorname{Arg} \max_{u_2 \in \mathcal{U}} J\left(\hat{u}_1, u_2\right) = \left\{\hat{u}_1\right\}.$$

Technically, these considerations are not totally rigorous for the classes of state-feedback strategies, since the corresponding lower and upper game values have to be defined by using specific mathematical constructions or hypotheses [5–8,30,52]. However, we can still adopt that a state-feedback strategy of cohort 1 is uninvadable if it gives the minimum in an appropriately defined upper (inf-sup) value of the game (13)–(15) and this value is nonpositive. Similarly, a state-feedback strategy of cohort 2 is said to be uninvadable if it gives the maximum in the related lower (sup-inf) value of the game (13)–(15) and this value is nonnegative. The same can be noted for the classes of nonanticipative strategies together with the corresponding lower and upper game values [23,57].

Thus, the aim to find uninvadable or evolutionary stable strategies of the pathogen cohorts leads to the differential game (13)–(15).

If a saddle pair of open-loop control strategies exists, then, under standard technical assumptions, it satisfies Pontryagin's minimax (or maximin) principle [57, Sect. 3.3]. Some sufficient conditions for existence of saddle open-loop control strategies were given in [24, 29,40,47–49]. However, they are rather strict and cannot be applied to the game (13)–(15).

Let V^{-}_{VREK} and V^{+}_{VREK} be the lower and upper value functions for the game (13)–(15) in the sense of nonanticipative strategies, respectively. Also let $V^{-}_{\text{s-f}}$ and $V^{+}_{\text{s-f}}$ be the lower and upper value functions for (13)–(15) that arise from the consideration of limit behavior of step-by-step control procedures based on state-feedback strategies [52, Sect. III.11]. These functions are defined for $(t, M_1, M_2) \in [0, T] \times G$ (since the states are restricted to lie in the strongly invariant domain G). The Hamiltonian

$$\begin{aligned} H(t, M_1, M_2, u_1, u_2, p_1, p_2) &\stackrel{\text{def}}{=} p_1 \left((1 - u_1)\, f_1(M_1, M_2) - g(M_1)\right) \\ &+ p_2 \left((1 - u_2)\, f_2(M_1, M_2) - g(M_2)\right) + e^{-\mu t} \left(u_2\, f_2(M_1, M_2) - u_1\, f_1(M_1, M_2)\right) \quad (18) \\ \forall t \in [0, T] \quad \forall\, (M_1, M_2) \in G \quad \forall\, (u_1, u_2) \in [0, 1]^2 \quad \forall\, (p_1, p_2) \in \mathbb{R}^2 \end{aligned}$$

for (13)–(15) obviously satisfies the Isaacs condition

$$\begin{aligned} &\min_{u_1 \in [0,1]} \max_{u_2 \in [0,1]} H(t, M_1, M_2, u_1, u_2, p_1, p_2) \\ &\quad = \max_{u_2 \in [0,1]} \min_{u_1 \in [0,1]} H(t, M_1, M_2, u_1, u_2, p_1, p_2) \stackrel{\text{def}}{=} \mathcal{H}(t, M_1, M_2, p_1, p_2) \\ &\forall t \in [0, T] \quad \forall\, (M_1, M_2) \in G \quad \forall\, (p_1, p_2) \in \mathbb{R}^2 \end{aligned}$$

(p_1 and p_2 are the adjoint variables or, in other words, costates). Then, according to [23, Sect. XI.6], the functions V^{-}_{VREK}, V^{+}_{VREK} coincide with each other and with the unique viscosity solution $V : [0, T] \times G \to \mathbb{R}$ to the following Cauchy problem for the Hamilton–Jacobi–Isaacs (or, in short, HJI) equation:

$$\begin{cases} -\dfrac{\partial V(t, M_1, M_2)}{\partial t} - \mathcal{H}\left(t, M_1, M_2, \dfrac{\partial V(t, M_1, M_2)}{\partial M_1}, \dfrac{\partial V(t, M_1, M_2)}{\partial M_2}\right) = 0, \\ V(T, M_1, M_2) = 0, \quad (M_1, M_2) \in G, \quad t \in [0, T]. \end{cases} \tag{19}$$

Due to [52, Theorem III.11.4 and Sect. I.4], we have $V^{-}_{\text{s-f}} = V^{+}_{\text{s-f}} = V$, and this is also the unique minimax solution to the problem

$$\begin{cases} \dfrac{\partial V(t, M_1, M_2)}{\partial t} + \mathcal{H}\left(t, M_1, M_2, \dfrac{\partial V(t, M_1, M_2)}{\partial M_1}, \dfrac{\partial V(t, M_1, M_2)}{\partial M_2}\right) = 0, \\ V(T, M_1, M_2) = 0, \quad (M_1, M_2) \in G, \quad t \in [0, T] \end{cases} \tag{20}$$

(several equivalent definitions of minimax solutions can be found in [52, Sect. I.3, I.4, II.6, II.7]).

In the particular case, when V is continuously differentiable everywhere on $[0, T] \times G$, the saddle state-feedback control strategies can be constructed from the inclusions

$$\begin{aligned} u_1(t, M_1, M_2) &\in \operatorname{Arg} \min_{w_1 \in [0,1]} \left\{ \max_{w_2 \in [0,1]} H\left(t, M_1, M_2, w_1, w_2, \right.\right. \\ &\left.\left. \frac{\partial V(t, M_1, M_2)}{\partial M_1}, \frac{\partial V(t, M_1, M_2)}{\partial M_2}\right)\right\}, \\ u_2(t, M_1, M_2) &\in \operatorname{Arg} \max_{w_2 \in [0,1]} \left\{ \min_{w_1 \in [0,1]} H\left(t, M_1, M_2, w_1, w_2, \right.\right. \\ &\left.\left. \frac{\partial V(t, M_1, M_2)}{\partial M_1}, \frac{\partial V(t, M_1, M_2)}{\partial M_2}\right)\right\} \\ &\forall t \in [0, T] \quad \forall\, (M_1, M_2) \in G \end{aligned}$$

(see [52, Sect. III.11.5]), which are simplified to

$$u_1(t, M_1, M_2) = \begin{cases} 0, & e^{-\mu t} + \frac{\partial V(t,M_1,M_2)}{\partial M_1} < 0, \\ 1, & e^{-\mu t} + \frac{\partial V(t,M_1,M_2)}{\partial M_1} > 0, \\ \text{arbitrary from } [0,1], & e^{-\mu t} + \frac{\partial V(t,M_1,M_2)}{\partial M_1} = 0, \end{cases}$$

$$u_2(t, M_1, M_2) = \begin{cases} 0, & e^{-\mu t} - \frac{\partial V(t,M_1,M_2)}{\partial M_2} < 0, \\ 1, & e^{-\mu t} - \frac{\partial V(t,M_1,M_2)}{\partial M_2} > 0, \\ \text{arbitrary from } [0,1], & e^{-\mu t} - \frac{\partial V(t,M_1,M_2)}{\partial M_2} = 0, \end{cases} \tag{21}$$

$$\forall t \in [0, T] \quad \forall (M_1, M_2) \in G.$$

Thus, the nonanticipative and state-feedback formulations of the differential game (13)–(15) are reduced to the Cauchy problem for the nonlinear first-order partial differential equation (19) or (20). One possible way to investigate this problem is to obtain the global field of its characteristics [5,6,8,34,52]. The method of characteristics (or, more precisely, an extension of the classical Cauchy method) is closely related to Pontryagin's principle, but some important features have to be emphasized. Contrary to optimal control problems, Pontryagin's principle for zero-sum two-player differential games provides necessary conditions only for saddle open-loop strategies, but not for saddle state-feedback strategies. The main qualitative difference in the behavior of characteristics for optimal control problems and differential games lies in the so-called corner conditions on switching manifolds [5–8]. While Pontryagin's theorem extends to optimal control theory, the Weierstrass–Erdmann condition states that the adjoint function is continuous along an extremal trajectory, and differential game theory does not exclude discontinuities there. These singularities in general cannot be found by a local analysis along isolated characteristics and require the construction of a complete field of extremals, leading to a global synthesis map. Recall also significant difficulties in verifying the existence of saddle open-loop strategies, as opposed to the well-known general result on the existence of saddle state-feedback strategies [4,30].

Our aim is to investigate the Cauchy problem (19) for the HJI equation by the method of characteristics in order to describe the corresponding state-feedback control strategies, and then to give reasonable biological interpretations. It is also useful to compare the related analytical results with the results of solving this problem by an entirely numerical method such as finite-difference approximation [12,15,23,39]. This can serve as a heuristic practical verification of our theoretical conjectures, while complete rigorous analysis of the global field of characteristics turns out to be very difficult.

3 Investigation of the Zero-Sum Two-Cohort Differential Game via the Method of Characteristics

From now on, Dieudonné's notation (4) will be actively used.

As is already mentioned in Sect. 2, the value function $V^-_{\text{VREK}} = V^+_{\text{VREK}} = V^-_{\text{s-f}} = V^+_{\text{s-f}}$ for the differential game (13)–(15) is described by the Cauchy problem (19) (or (20)) for the HJI equation in the finite-horizon case. Let us investigate this problem for $T < +\infty$ by the method of characteristics [5,6,8,34,52]. Although Pontryagin's minimax principle [57, Sect. 3.3] is in general not a necessary condition for a saddle pair of nonanticipative or

state-feedback control strategies, the corresponding characteristic (state dynamic and adjoint) equations

$$\begin{cases} \dfrac{\mathrm{d}M_1(t)}{\mathrm{d}t} = (1-u_1(t))\, f_1(M_1(t), M_2(t)) - g(M_1(t)), \\ \dfrac{\mathrm{d}M_2(t)}{\mathrm{d}t} = (1-u_2(t))\, f_2(M_1(t), M_2(t)) - g(M_2(t)), \end{cases} \tag{22}$$

$$\begin{cases} \dfrac{\mathrm{d}p_1(t)}{\mathrm{d}t} = -\dfrac{\partial H(t,\, M_1(t),\, M_2(t),\, u_1(t),\, u_2(t),\, p_1(t),\, p_2(t))}{\partial M_1} \\ \quad = p_1(t)\,(g'(M_1(t)) - (1-u_1(t))\,\mathrm{D}_1 f_1(M_1(t), M_2(t))) \\ \quad\quad -p_2(t)\,(1-u_2(t))\,\mathrm{D}_1 f_2(M_1(t), M_2(t)) \\ \quad\quad +e^{-\mu t}\,(u_1(t)\,\mathrm{D}_1 f_1(M_1(t), M_2(t)) - u_2(t)\,\mathrm{D}_1 f_2(M_1(t), M_2(t))), \\ \dfrac{\mathrm{d}p_2(t)}{\mathrm{d}t} = -\dfrac{\partial H(t,\, M_1(t),\, M_2(t),\, u_1(t),\, u_2(t),\, p_1(t),\, p_2(t))}{\partial M_2} \\ \quad = p_2(t)\,(g'(M_2(t)) - (1-u_2(t))\,\mathrm{D}_2 f_2(M_1(t), M_2(t))) \\ \quad\quad -p_1(t)\,(1-u_1(t))\,\mathrm{D}_2 f_1(M_1(t), M_2(t)) \\ \quad\quad +e^{-\mu t}\,(u_1(t)\,\mathrm{D}_2 f_1(M_1(t), M_2(t)) - u_2(t)\,\mathrm{D}_2 f_2(M_1(t), M_2(t))), \\ p_1(T) = p_2(T) = 0, \end{cases} \tag{23}$$

together with the Hamiltonian saddle-point condition

$$\begin{aligned} u_1(t) &\in \operatorname{Arg}\min_{v_1\in[0,1]} \left\{ \max_{v_2\in[0,1]} H(t,\, M_1(t),\, M_2(t),\, v_1,\, v_2,\, p_1(t),\, p_2(t)) \right\}, \\ u_2(t) &\in \operatorname{Arg}\max_{v_2\in[0,1]} \left\{ \min_{v_1\in[0,1]} H(t,\, M_1(t),\, M_2(t),\, v_1,\, v_2,\, p_1(t),\, p_2(t)) \right\} \end{aligned}$$

can still be used for the global analysis of (19), but not just for the analysis of isolated characteristics (recall the related discussion in the end of Sect. 2). With the help of formula (18), the latter inclusions are simplified to

$$u_1(t) = \begin{cases} 0, & e^{-\mu t} + p_1(t) < 0, \\ 1, & e^{-\mu t} + p_1(t) > 0, \\ \text{arbitrary from } [0,1], & e^{-\mu t} + p_1(t) = 0, \end{cases} \tag{24}$$

$$u_2(t) = \begin{cases} 0, & e^{-\mu t} - p_2(t) < 0, \\ 1, & e^{-\mu t} - p_2(t) > 0, \\ \text{arbitrary from } [0,1], & e^{-\mu t} - p_2(t) = 0. \end{cases} \tag{25}$$

Since the boundary conditions for the adjoint variables p_1, p_2 are imposed at $t = T$, it is convenient to rewrite (22)–(25) in reverse time $\tau \overset{\text{def}}{=} T - t$:

$$\begin{cases} \dfrac{\mathrm{d}M_1}{\mathrm{d}\tau} = g(M_1) - (1-u_1)\, f_1(M_1, M_2), \\ \dfrac{\mathrm{d}M_2}{\mathrm{d}\tau} = g(M_2) - (1-u_2)\, f_2(M_1, M_2), \end{cases} \tag{26}$$

$$\begin{cases} \dfrac{\mathrm{d}p_1}{\mathrm{d}\tau} = -\,p_1\,g'(M_1) + p_1\,\mathrm{D}_1 f_1(M_1,M_2) + p_2\,\mathrm{D}_1 f_2(M_1,M_2) \\ \qquad\qquad - \left(e^{-\mu\,(T-\tau)} + p_1\right) u_1\,\mathrm{D}_1 f_1(M_1,M_2) \\ \qquad\qquad + \left(e^{-\mu\,(T-\tau)} - p_2\right) u_2\,\mathrm{D}_1 f_2(M_1,M_2), \\ \dfrac{\mathrm{d}p_2}{\mathrm{d}\tau} = -\,p_2\,g'(M_2) + p_1\,\mathrm{D}_2 f_1(M_1,M_2) + p_2\,\mathrm{D}_2 f_2(M_1,M_2) \\ \qquad\qquad - \left(e^{-\mu\,(T-\tau)} + p_1\right) u_1\,\mathrm{D}_2 f_1(M_1,M_2) \\ \qquad\qquad + \left(e^{-\mu\,(T-\tau)} - p_2\right) u_2\,\mathrm{D}_2 f_2(M_1,M_2), \\ p_1\,|_{\tau=0} = p_2\,|_{\tau=0} = 0, \end{cases} \tag{27}$$

$$u_1 = \begin{cases} 0, & e^{-\mu\,(T-\tau)} + p_1 < 0, \\ 1, & e^{-\mu\,(T-\tau)} + p_1 > 0, \\ \text{arbitrary from } [0,1], & e^{-\mu\,(T-\tau)} + p_1 = 0, \end{cases} \tag{28}$$

$$u_2 = \begin{cases} 0, & e^{-\mu\,(T-\tau)} - p_2 < 0, \\ 1, & e^{-\mu\,(T-\tau)} - p_2 > 0, \\ \text{arbitrary from } [0,1], & e^{-\mu\,(T-\tau)} - p_2 = 0. \end{cases} \tag{29}$$

Here the time argument for $M_1, M_2, u_1, u_2, p_1, p_2$ is not shown for brevity.

Formulas (28),(29) together with the boundary conditions for the adjoint system (27) directly imply that $u_1 = u_2 = 1$ for sufficiently small τ (or, equivalently, for t sufficiently close to T).

3.1 Singular Control Regimes for Both Cohorts

First, let us study the situation when, on some time subinterval, we have $e^{-\mu\,(T-\tau)} + p_1 = e^{-\mu\,(T-\tau)} - p_2 = 0$, i.e., when singular control regimes take place simultaneously for both cohorts.

From (27), we get

$$\begin{aligned} &\frac{\mathrm{d}}{\mathrm{d}\tau}\left(e^{-\mu\,(T-\tau)} + p_1\right)\Big|_{e^{-\mu\,(T-\tau)}+p_1=0} \\ &\quad = -e^{-\mu\,(T-\tau)}\left(\mathrm{D}_1 f_1(M_1,M_2) - g'(M_1) - \mu\right) \\ &\qquad + \; p_2\,\mathrm{D}_1 f_2(M_1,M_2) + \left(e^{-\mu\,(T-\tau)} - p_2\right) u_2\,\mathrm{D}_1 f_2(M_1,M_2), \end{aligned} \tag{30}$$

$$\begin{aligned} &\frac{\mathrm{d}}{\mathrm{d}\tau}\left(e^{-\mu\,(T-\tau)} - p_2\right)\Big|_{e^{-\mu\,(T-\tau)}-p_2=0} \\ &\quad = -e^{-\mu\,(T-\tau)}\left(\mathrm{D}_2 f_2(M_1,M_2) - g'(M_2) - \mu\right) \\ &\qquad - \; p_1\,\mathrm{D}_2 f_1(M_1,M_2) + \left(e^{-\mu\,(T-\tau)} + p_1\right) u_1\,\mathrm{D}_2 f_1(M_1,M_2), \end{aligned} \tag{31}$$

and, therefore,

$$\begin{aligned}
&\frac{\mathrm{d}}{\mathrm{d}\tau}\left(e^{-\mu(T-\tau)}+p_1\right)\Big|_{e^{-\mu(T-\tau)}+p_1=e^{-\mu(T-\tau)}-p_2=0}\\
&\quad=-e^{-\mu(T-\tau)}\left(\mathrm{D}_1[f_1-f_2](M_1,M_2)-g'(M_1)-\mu\right),\\
&\frac{\mathrm{d}}{\mathrm{d}\tau}\left(e^{-\mu(T-\tau)}-p_2\right)\Big|_{e^{-\mu(T-\tau)}+p_1=e^{-\mu(T-\tau)}-p_2=0}\\
&\quad=-e^{-\mu(T-\tau)}\left(\mathrm{D}_2[f_2-f_1](M_1,M_2)-g'(M_2)-\mu\right).
\end{aligned}$$

Thus, singular control regimes can appear simultaneously for the two cohorts only when

$$\mathrm{D}_1[f_1-f_2](M_1,M_2)-g'(M_1)=\mathrm{D}_2[f_2-f_1](M_1,M_2)-g'(M_2)=\mu. \tag{32}$$

Due to the form of the nutrient fluxes given in Assumption 2.3, equations (32) transform into

$$\begin{aligned}
&n_1\,\nu'(n_1M_1+n_2M_2)\,(\rho(M_1)-\rho(M_2))+\nu(n_1M_1+n_2M_2)\,\rho'(M_1)-g'(M_1)\\
&\quad=\ n_2\,\nu'(n_1M_1+n_2M_2)\,(\rho(M_2)-\rho(M_1))+\nu(n_1M_1+n_2M_2)\,\rho'(M_2)-g'(M_2)\\
&\quad=\ \mu.
\end{aligned} \tag{33}$$

Denote

$$\begin{aligned}
n &\stackrel{\text{def}}{=} n_1+n_2,\\
f(M) &\stackrel{\text{def}}{=} f_1(M,M)=f_2(M,M)=\nu(nM)\,\rho(M)\quad\forall M\geqslant 0.
\end{aligned}$$

For establishing the next result on the concurrent singular control regimes, one also needs the properties of the functions $\nu(\cdot)$, $\rho(\cdot)$, $g(\cdot)$ from Assumption 2.4.

Theorem 3.1 *Suppose that $T<+\infty$ and Assumptions 2.1–2.4 hold. The system of equations (33) with respect to (M_1,M_2) has a unique solution $(M^{**},M^{**})\in G$, where M^{**} is a unique root of the equation*

$$\nu(nM^{**})\,\rho'(M^{**})-g'(M^{**})=\mu \tag{34}$$

on $\left(0,\bar{M}_{\min}\right)$. Consider a solution to the reverse-time characteristic system (26)–(29) with $(M_1,M_2)|_{\tau=0}\in G$ on the maximum subinterval of $[0,T]$ where the state stays in G. Singular control regimes may take place simultaneously for both cohorts only when $M_1=M_2=M^{**}$ and $u_1=u_2=u^{**}\in[0,1]$, where

$$u^{**}\ \stackrel{\text{def}}{=}\ 1-\frac{g(M^{**})}{f(M^{**})}\,. \tag{35}$$

Moreover, if $\bar{M}_1=\bar{M}_2\stackrel{\text{def}}{=}\bar{M}$ and the equation

$$\begin{aligned}
&f'(M^*)-g'(M^*)\\
&\quad=\ n\,\nu'(nM^*)\,\rho(M^*)+\nu(nM^*)\,\rho'(M^*)-g'(M^*)=\mu
\end{aligned} \tag{36}$$

has a unique root $M^*\in\left(0,\bar{M}\right)$ (which is related to singular arcs in the optimal control problem (11), (12) according to Assumption A.2 and Proposition A.3 in Online Appendix A), then

$$\begin{aligned}
&M^*\leqslant M^{**},\\
&(n>0,\ \ \nu'(nM^*)<0)\ \Longrightarrow\ (M^*<M^{**}).
\end{aligned} \tag{37}$$

Proof From equations (33), we obtain

$$n\,\nu'(n_1M_1+n_2M_2)\,(\rho(M_2)-\rho(M_1))$$
$$+\nu(n_1M_1+n_2M_2)\,(\rho'(M_2)-\rho'(M_1))+(g'(M_1)-g'(M_2))=0.$$

With the help of items 1–5 of Assumption 2.4, one can directly verify that, in the domain (2), this equality can hold only for $M_1 = M_2$ (its left-hand side is negative for $M_1 < M_2$ and positive for $M_1 > M_2$). Then system (33) is reduced to one equation (34). By using items 1–5 of Assumption 2.4 again, we get

$$\begin{aligned}&\frac{\partial}{\partial M}\left(\nu(nM)\,\rho'(M)-g'(M)\right)\\&\qquad=\ n\,\nu'(nM)\,\rho'(M)+\nu(nM)\,\rho''(M)-g''(M)<0\\&\forall M\in\left(0,\,\bar{M}_{\max}\right).\end{aligned}\tag{38}$$

Together with the final items 6,7, this leads to the existence of a unique root M^{**} of (34) on $\left(0,\,\bar{M}_{\min}\right)$. Thus, $(M^{**},\,M^{**})$ is a unique solution to (33) in G, and the control strategies u_1, u_2 may act in singular regimes simultaneously only when $M_1 = M_2 = M^{**}$ and $u_1 = u_2 = u^{**} \in [0,\,1]$.

It remains to verify the properties (37). From equations (34),(36) together with item 1 of Assumption 2.4, we obtain

$$\nu(nM^*)\,\rho'(M^*)-g'(M^*)\geqslant\nu(nM^{**})\,\rho'(M^{**})-g'(M^{**}).\tag{39}$$

According to (38), this implies $M^* \leqslant M^{**}$. If we also have $n > 0$ and $\nu'(nM^*) < 0$, then the inequality (39) becomes strict and, therefore, $M^* < M^{**}$. □

Remark 3.2 The inequality $M^* < M^{**}$ means that, in comparison with the singular control regime in the single-cohort optimization problem, maintaining the singular control regime for both cohorts in the zero-sum differential game requires greater resources. □

The next assumption is imposed in order to have $0 < u^{**} < 1$, i.e., an intermediate configuration of resource allocation in the singular control regime for the two cohorts.

Assumption 3.3 $f(M^{**}) > g(M^{**})$.

Example 3.4 Let $n \geqslant 0$, and let the representations (5)–(7) hold with positive constants α, k, β, γ satisfying the inequality (8). Then Assumptions 2.1, 2.3–2.6 are fulfilled (see Example 2.8). Assumption 2.2 is trivial and supposed to hold *a priori*. Hence, Theorem 3.1 can be applied. If $n > 0$, then $\nu'(\cdot)$ is negative on $[0, +\infty)$ and, by virtue of (37), $M^* < M^{**}$. Finally, note that (34) transforms into

$$\frac{1}{1+\beta n M^{**}}\,\alpha\,\frac{k}{(M^{**}+k)^2}=\gamma+\mu,$$

which implies fulfillment of Assumption 3.3:

$$f(M^{**})=\frac{1}{1+\beta n M^{**}}\,\frac{\alpha M^{**}}{M^{**}+k}=(\gamma+\mu)\,M^{**}\,\frac{M^{**}+k}{k}>\gamma M^{**}=g(M^{**}).$$

Therefore, the singular control (35) is admissible and specifies an intermediate configuration of resource allocation. □

3.2 Characteristics in Case $M_1\,|_{\tau=0} \neq M_2\,|_{\tau=0}$

In this subsection, we need to adopt the linear form (7) for the function $g(\cdot)$.

Assumption 3.5 $g(M) = \gamma M$ for all $M \geqslant 0$, γ is a positive constant.

The next theorem describes important properties of solutions to the reverse-time characteristic system (26)–(29) in case $M_1\,|_{\tau=0} \neq M_2\,|_{\tau=0}$ (or, equivalently, $M_1\,|_{t=T} \neq M_2\,|_{t=T}$).

Theorem 3.6 *Suppose that $T < +\infty$ and Assumptions 2.1–2.4, 3.5 hold. Consider a solution to the reverse-time characteristic system (26)–(29) with $(M_1, M_2)\,|_{\tau=0} \in G$ on the maximum subinterval $I \subseteq [0, T]$ where the state stays in G. Let $\mathcal{T}$ be the right endpoint of I (in fact, $I = [0, T]$ if $\mathcal{T} = T$ and $(M_1, M_2)\,|_{\tau=T} \in G$, otherwise $I = [0, \mathcal{T})$). Fix an arbitrary instant $\tau' \in [0, \mathcal{T})$ and denote*

$$[\tau', \mathcal{T}\} \stackrel{\text{def}}{=} [\tau', T] \cap I, \quad (\tau', \mathcal{T}\} \stackrel{\text{def}}{=} (\tau', T] \cap I$$

(where $\}$ is either $]$ or $)$ depending on I). Then the following implications hold:

$$\begin{aligned}
&(M_1\,|_{\tau=\tau'} > M_2\,|_{\tau=\tau'}\,, \quad (p_1 + p_2)\,|_{\tau=\tau'} \geqslant 0)\\
&\quad \Longrightarrow \quad \big(M_1 > M_2 \quad \forall \tau \in [\tau', \mathcal{T}\}, \quad p_1 + p_2 > 0 \quad \forall \tau \in (\tau', \mathcal{T}\}\big)\,,\\
&(M_1\,|_{\tau=\tau'} < M_2\,|_{\tau=\tau'}\,, \quad (p_1 + p_2)\,|_{\tau=\tau'} \leqslant 0)\\
&\quad \Longrightarrow \quad \big(M_1 < M_2 \quad \forall \tau \in [\tau', \mathcal{T}\}, \quad p_1 + p_2 < 0 \quad \forall \tau \in (\tau', \mathcal{T}\}\big)\,.
\end{aligned}$$

In the particular case $\tau' = 0$, we have

$$\begin{aligned}
&(M_1\,|_{\tau=0} > M_2\,|_{\tau=0})\\
&\quad \Longrightarrow \quad (M_1 > M_2 \quad \forall \tau \in [0, \mathcal{T}\}, \quad p_1 + p_2 > 0 \quad \forall \tau \in (0, \mathcal{T}\})\,,
\end{aligned} \tag{40}$$

$$\begin{aligned}
&(M_1\,|_{\tau=0} < M_2\,|_{\tau=0})\\
&\quad \Longrightarrow \quad (M_1 < M_2 \quad \forall \tau \in [0, \mathcal{T}\}, \quad p_1 + p_2 < 0 \quad \forall \tau \in (0, \mathcal{T}\})\,.
\end{aligned} \tag{41}$$

Theorem 3.6 is proved in Section B.1 of Online Appendix B.

Remark 3.7 Consider a solution to the characteristic system (26)–(29) for $\tau \in [0, \mathcal{T}\}$ under the conditions of Theorem 3.6. Recall that $u_1 = u_2 = 1$ for sufficiently small τ (*i. e.*, for t sufficiently close to T). If $M_1\,|_{\tau=0} > M_2\,|_{\tau=0}$, then, due to (40), we have $e^{-\mu\,(T-\tau)} + p_1 > e^{-\mu\,(T-\tau)} - p_2$ for all $\tau \in (0, \mathcal{T}\}$, which, in particular, implies that, in reverse time, the first switching of u_1 may happen only after the first switching of u_2 (i.e., in forward time, the last switching of u_2 may happen only after the last switching of u_1). Similarly, if $M_1\,|_{\tau=0} < M_2\,|_{\tau=0}$, then, due to (41), $e^{-\mu\,(T-\tau)} + p_1 < e^{-\mu\,(T-\tau)} - p_2$ for all $\tau \in (0, \mathcal{T}\}$, which, in particular, implies that, in reverse time, the first switching of u_2 may happen only after the first switching of u_1 (i.e., in forward time, the last switching of u_1 may happen only after the last switching of u_2). □

3.3 Characteristics in Case $M_1\,|_{\tau=0} = M_2\,|_{\tau=0}$

In this subsection, we study solutions to the characteristic system (26)–(29) in case $M_1\,|_{\tau=0} = M_2\,|_{\tau=0}$.

3.3.1 Staying on the Plane $M_1 = M_2$

First, it is reasonable to describe the field of characteristics staying on the plane $M_1 = M_2$ under the action of equal control strategies $u_1 = u_2$. Then we arrive at the following system for $M_1 = M_2 = M$, $-p_1 = p_2 = p$, $u_1 = u_2 = u$:

$$\begin{cases} \dfrac{\mathrm{d}M}{\mathrm{d}\tau} = g(M) - (1-u)\, f(M), \\ \dfrac{\mathrm{d}p}{\mathrm{d}\tau} = -p\, g'(M) + \left(p + \left(e^{-\mu\,(T-\tau)} - p\right) u\right)\, \nu(nM)\, \rho'(M), \\ p\,|_{\tau=0} \;= 0, \\ u = \begin{cases} 0, & e^{-\mu\,(T-\tau)} - p < 0, \\ 1, & e^{-\mu\,(T-\tau)} - p > 0, \\ \text{arbitrary from } [0,\,1], & e^{-\mu\,(T-\tau)} - p = 0. \end{cases} \end{cases} \tag{42}$$

It can be investigated similarly to the characteristic system for the optimal control problem (11),(12). (The latter is studied in Online Appendix A.) That is why we omit the proofs of Proposition 3.9 and Theorem 3.11.

For the analysis of system (42), we do not need linearity of $g(\cdot)$, i.e., Assumption 3.5. The latter will be required further, when applying Theorem 3.6 to the reverse-time characteristics that leave the plane $M_1 = M_2$.

Here we impose a stronger condition than $f(M^{**}) > g(M^{**})$ in Assumption 3.3, and also positivity of $\rho'(M^{**})$.

Assumption 3.8 $f(M) > g(M)$ for all $M \in (0,\, M^{**}]$, and $\rho'(M^{**}) > 0$.

According to item 2 of Assumption 2.4, the inequality $\rho'(M^{**}) > 0$ implies that

$$\rho'(M) > 0 \quad \forall M \in [0,\, M^{**}]. \tag{43}$$

Similarly to Online Appendix A, we will indicate the feedback control law for system (42) on the plane $(t,\, M)$.

For describing the set of bang–bang switchings on the plane $(t,\, M)$, we need an auxiliary notation, as in Proposition A.6 of Online Appendix A. Fix arbitrary $\tau' \geqslant 0$ and $M' \in \left(0,\, \bar{M}_{\min}\right)$. Let us write the state dynamic equation from system (42) in reverse time for $u \equiv 1$:

$$\frac{\mathrm{d}M}{\mathrm{d}\tau} = g(M).$$

By $\eta(\cdot;\, \tau',\, M')$, denote its solution considered for $\tau \leqslant \tau'$ and reaching $M = M'$ at $\tau = \tau'$. Since this differential equation is autonomous, we have $\eta(\tau;\, \tau',\, M') = \eta(-(\tau' - \tau);\; 0,\, M')$ for all $\tau \leqslant \tau'$. In case $M' = 0$, we trivially set $\eta(\tau;\, \tau',\, 0) = 0$ for all $\tau \leqslant \tau'$ (because $g(0) = 0$ in line with item 4 of Assumption 2.1).

Proposition 3.9 *Suppose that $T < +\infty$ and Assumptions 2.1–2.4, 3.3, 3.8 hold. On the plane $(t,\, M)$, the bang–bang switching set for system (42) can be represented as*

$$\tilde{\Gamma}_{\text{b-b}} = \left\{(t,\, M) \;\in\; (-\infty,\, T] \times [0,\, M^{**}] :\; \tilde{\lambda}_{\text{b-b}}(T - t,\, M) \;= 0\right\},$$

where

$$\tilde{\lambda}_{\text{b-b}}(\tau, M) \stackrel{\text{def}}{=} 1 - \int_0^\tau \exp\left\{ - \int_0^s g'(\eta(-\xi; 0, M))\, d\xi - \mu s \right\} \cdot \nu(n\, \eta(-s; 0, M))\, \rho'(\eta(-s; 0, M))\, ds \tag{44}$$
$$\forall \tau \geqslant 0 \quad \forall M \in \left[0, \bar{M}_{\min}\right).$$

For $M \neq 0$, formula (44) can be simplified to

$$\tilde{\lambda}_{\text{b-b}}(\tau, M) = 1 - \frac{1}{g(M)} \int_0^\tau e^{-\mu s}\, g(\eta(-s; 0, M))\, \nu(n\, \eta(-s; 0, M))\, \rho'(\eta(-s; 0, M))\, ds$$
$$\forall \tau \geqslant 0 \quad \forall M \in \left(0, \bar{M}_{\min}\right),$$

as in Remark A.8 of Online Appendix A.

From relations (43), (44) and the fact that $0 \leqslant \eta(-\tau; 0, M) \leqslant M$ for all $\tau \geqslant 0$ and $M \in \left[0, \bar{M}_{\min}\right)$, we get

$$\frac{\partial \tilde{\lambda}_{\text{b-b}}(\tau, M)}{\partial \tau} = -\exp\left\{ - \int_0^\tau g'(\eta(-\xi; 0, M))\, d\xi - \mu\tau \right\} \cdot \nu(n\, \eta(-\tau; 0, M))\, \rho'(\eta(-\tau; 0, M)) < 0 \tag{45}$$
$$\forall \tau \geqslant 0 \quad \forall M \in [0, M^{**}].$$

The role of the next assumption is similar to the role of Assumption A.7 in Online Appendix A.

Assumption 3.10 For any $M \in (0, M^{**}]$, there exists a number $\tau > 0$ satisfying $\tilde{\lambda}_{\text{b-b}}(\tau, M) = 0$, or, equivalently,

$$\int_0^{+\infty} e^{-\mu s}\, g(\eta(-s; 0, M))\, \nu(n\, \eta(-s; 0, M))\, \rho'(\eta(-s; 0, M))\, ds > g(M) \tag{46}$$
$$\forall M \in (0, M^{**}].$$

Similarly to the reasoning in the end of Remark A.8 in Online Appendix A, one can use formula (44) and item 6 of Assumption 2.4 in order to show that the case $M = 0$ does not need to be included in Assumption 3.10.

The inequality (45) implies uniqueness of τ in Assumption 3.10 and also the fact that $\tilde{\Gamma}_{\text{b-b}}$ is a regular curve. In particular, there exists a unique $\tau^{**} > 0$ satisfying $\tilde{\lambda}_{\text{b-b}}(\tau^{**}, M^{**}) = 0$. Furthermore, if we consider the curve $\tilde{\Gamma}_{\text{b-b}}$ in reverse time, then it will not depend on the finite time horizon T. The numbers M^{**}, τ^{**} are also independent from T.

Similarly to Assumption A.7 in Online Appendix A, analytical verification of Assumption 3.10 may be rather complicated, but a practical test for the corresponding condition (46) is naturally implemented within the numerical construction of $\tilde{\Gamma}_{\text{b-b}}$, when computing zeros of (44).

Similarly to Remark A.11 in Online Appendix A, Assumptions 2.1–2.4, 3.3, 3.8, 3.10 guarantee transversal crossing of the bang–bang switching curve $\tilde{\Gamma}_{\text{b-b}}$ by the characteristic arcs of (42) with $u = 0$.

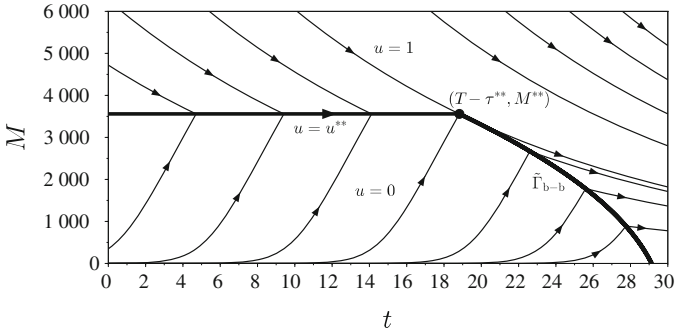

(a) The portrait on the plane (t, M)

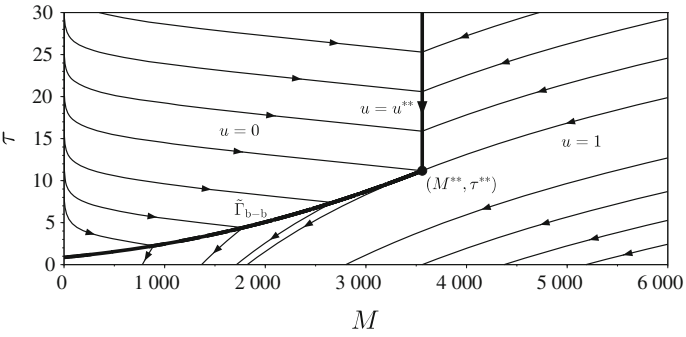

(b) The portrait on the plane (M, τ)

Fig. 2 The feedback control law (47) for the time horizon $T = 30$, functions (5)–(7), and parameter values (10). The portrait is drawn (**a**) on the plane (t, M) and (**b**) on the plane (M, τ). The arrows on the trajectories correspond to the forward-time directions

The above notation allows us to formulate a result on the structure of the feedback control strategy for system (42) (recall Theorem A.12 in Online Appendix A and see also Fig. 2a).

Theorem 3.11 *Suppose that $T < +\infty$ and Assumptions 2.1–2.4, 3.3, 3.8, 3.10 hold. The field of the characteristics staying on the plane $M_1 = M_2$ and governed by system (42) determines the following feedback control strategy*:

$$u(t, M) = \begin{cases} 1, & 0 < M < M^{**},\ \tilde{\lambda}_{\text{b-b}}(T - t, M) \geqslant 0, \\ 0, & 0 < M < M^{**},\ \tilde{\lambda}_{\text{b-b}}(T - t, M) < 0, \\ u^{**}, & M = M^{**},\ 0 \leqslant t < T - \tau^{**}, \\ 1, & M = M^{**},\ T - \tau^{**} \leqslant t \leqslant T, \\ 1, & M > M^{**}, \end{cases} \tag{47}$$

$$\forall t \in [0, T] \quad \forall M \in \left(0, \bar{M}_{\min}\right).$$

Figure 2a illustrates the constructed feedback control law for the time horizon $T = 30$, functions (5)–(7), and parameter values (10) (which satisfy Assumptions 2.1, 2.3–2.6, 3.3, 3.5, 3.8, 3.10). For further reverse-time considerations, it is also useful to draw the related

portrait of characteristics on the plane (M, τ), as done in Fig. 2b (where the arrows on the trajectories still correspond to the forward-time directions).

3.3.2 Exit from the Plane $M_1 = M_2$

The next step is to describe the reverse-time characteristics that start from $M_1|_{\tau=0} = M_2|_{\tau=0}$ and leave the plane $M_1 = M_2$ when reaching suitable positions. This leaving can happen only as a result of such control switchings that make $u_1 \neq u_2$ without violation of the Hamiltonian saddle-point condition (28), (29). The above analysis of the system (42) implies that it is possible to stop staying on the plane $M_1 = M_2$ only at the positions

$$\begin{aligned} &(\tau, M_1, M_2, p_1, p_2) = \left(\tau', M^{**}, M^{**}, -e^{-\mu(T-\tau')}, e^{-\mu(T-\tau')}\right), \\ &\tau^{**} \leqslant \tau' < T. \end{aligned} \tag{48}$$

Suppose that $\tau^{**} < T$, and let $\tau' \in [\tau^{**}, T)$ be such an exit instant. Then, in some right neighborhood of $\tau = \tau'$, the following regimes are possible:

(1) $u_1 = 1, u_2$ is singular, $M_1 > M_2, e^{-\mu(T-\tau)} + p_1 > 0, e^{-\mu(T-\tau)} - p_2 = 0, p_1 + p_2 > 0$;
(2) u_1 is singular, $u_2 = 1, M_1 < M_2, e^{-\mu(T-\tau)} + p_1 = 0, e^{-\mu(T-\tau)} - p_2 > 0, p_1 + p_2 < 0$;
(3) u_1 is singular, $u_2 = 0, M_1 > M_2, e^{-\mu(T-\tau)} + p_1 = 0, e^{-\mu(T-\tau)} - p_2 < 0, p_1 + p_2 > 0$;
(4) $u_1 = 0, u_2$ is singular, $M_1 < M_2, e^{-\mu(T-\tau)} + p_1 < 0, e^{-\mu(T-\tau)} - p_2 = 0, p_1 + p_2 < 0$;
(5) $u_1 = 1, u_2 = 0, M_1 > M_2, e^{-\mu(T-\tau)} + p_1 > 0, e^{-\mu(T-\tau)} - p_2 < 0, p_1 + p_2 > 0$;
(6) $u_1 = 0, u_2 = 1, M_1 < M_2, e^{-\mu(T-\tau)} + p_1 < 0, e^{-\mu(T-\tau)} - p_2 > 0, p_1 + p_2 < 0$.

Let Assumption 3.5 hold in addition to $T < +\infty$ and Assumptions 2.1–2.4, 3.3, 3.8, 3.10. By using Theorem 3.6, we conclude that, if the regime 1, 3, or 5 takes place in some right neighborhood of $\tau = \tau'$, then $M_1 > M_2$ and $p_1 + p_2 > 0$ for all $\tau \in (\tau', \mathcal{T}\}$. Similarly, if regime 2, 4, or 6 takes place in some right neighborhood of $\tau = \tau'$, then $M_1 < M_2$ and $p_1 + p_2 < 0$ for all $\tau \in (\tau', \mathcal{T}\}$.

The regular regimes 5 and 6 do not need to be separately investigated, because the corresponding control values are known *a priori*. Let us characterize the singular control components for regimes 1–4.

3.3.2.1 *Singular control regimes* 1–4

Regime 1 By virtue of the representation (31), we have

$$\begin{aligned} &\frac{\mathrm{d}}{\mathrm{d}\tau}\left(e^{-\mu(T-\tau)} - p_2\right)\Big|_{e^{-\mu(T-\tau)} - p_2 = 0,\ u_1 = 1} \\ &\quad = -e^{-\mu(T-\tau)}\left(\mathrm{D}_2[f_2 - f_1](M_1, M_2) - g'(M_2) - \mu\right), \end{aligned}$$

which implies

$$\mathrm{D}_2[f_2 - f_1](M_1, M_2) - g'(M_2) - \mu = 0 \tag{49}$$

due to singularity of the control u_2. By differentiating the last equality with respect to τ subject to the state dynamic equations (26) for $u_1 = 1$, we can find the corresponding feedback control law $u_2 = u_2(M_1, M_2)$:

$$\begin{aligned} &\mathrm{D}_{12}[f_2 - f_1](M_1, M_2)\, g(M_1) + (\mathrm{D}_{22}[f_2 - f_1](M_1, M_2) - g''(M_2)) \\ &\quad \cdot\, (g(M_2) - (1 - u_2)\, f_2(M_1, M_2)) = 0, \end{aligned} \tag{50}$$

$$(1 - u_2)\, f_2(M_1, M_2) - g(M_2) = \; g(M_1)\, \frac{\mathrm{D}_{12}[f_2 - f_1](M_1, M_2)}{\mathrm{D}_{22}[f_2 - f_1](M_1, M_2) - g''(M_2)}\,.$$

Regime 2 Similarly to the reasonings for regime 1, we consecutively derive

$$\mathrm{D}_1[f_1 - f_2](M_1, M_2) - g'(M_1) - \mu = 0, \tag{51}$$

$$\begin{aligned} &\mathrm{D}_{12}[f_1 - f_2]\, g(M_2) + (\mathrm{D}_{11}[f_1 - f_2](M_1, M_2) - g''(M_1)) \\ &\quad \cdot\, (g(M_1) - (1 - u_1)\, f_1(M_1, M_2)) = 0, \end{aligned} \tag{52}$$

$$(1 - u_1)\, f_1(M_1, M_2) - g(M_1) = \; g(M_2)\, \frac{\mathrm{D}_{12}[f_1 - f_2](M_1, M_2)}{\mathrm{D}_{11}[f_1 - f_2](M_1, M_2) - g''(M_1)}\,.$$

Regime 3 From the representation (30), we get

$$\begin{aligned} &\frac{\mathrm{d}}{\mathrm{d}\tau}\left(e^{-\mu\,(T-\tau)} + p_1\right)\Big|_{e^{-\mu\,(T-\tau)}+p_1=0,\;\; (e^{-\mu\,(T-\tau)}-p_2)\,u_2=0} \\ &\quad = -e^{-\mu\,(T-\tau)}\,(\mathrm{D}_1 f_1(M_1, M_2) - g'(M_1) - \mu) + p_2\,\mathrm{D}_1 f_2(M_1, M_2), \end{aligned}$$

i. e.,

$$p_2\,\mathrm{D}_1 f_2(M_1, M_2) - e^{-\mu\,(T-\tau)}\,(\mathrm{D}_1 f_1(M_1, M_2) - g'(M_1) - \mu) = 0 \tag{53}$$

due to singularity of the control u_1. In the degenerate case $n_1 = 0$, we have $\mathrm{D}_1 f_2(M_1, M_2) \equiv 0$ and thereby arrive at the relations

$$\mathrm{D}_1 f_1(M_1, M_2) - g'(M_1) - \mu = 0, \tag{54}$$

$$\begin{aligned} &(\mathrm{D}_{11} f_1(M_1, M_2) - g''(M_1))\,(g(M_1) - (1 - u_1)\, f_1(M_1, M_2)) \\ &\quad +\;\; \mathrm{D}_{12} f_1(M_1, M_2)\,(g(M_2) - f_2(M_1, M_2)) = 0, \end{aligned} \tag{55}$$

$$\begin{aligned} &(1 - u_1)\, f_1(M_1, M_2) - g(M_1) \\ &\qquad = \; \frac{\mathrm{D}_{12} f_1(M_1, M_2)\,(g(M_2) - f_2(M_1, M_2))}{\mathrm{D}_{11} f_1(M_1, M_2) - g''(M_1)}\,. \end{aligned}$$

Now suppose that $\mathrm{D}_1 f_2(M_1, M_2) \neq 0$ on the considered subarc. Then (53) gives

$$p_2 = e^{-\mu\,(T-\tau)}\,\frac{\mathrm{D}_1 f_1(M_1, M_2) - g'(M_1) - \mu}{\mathrm{D}_1 f_2(M_1, M_2)}\,. \tag{56}$$

By differentiating (53) with respect to τ subject to the equations (26),(27) for $u_2 = 0$, we obtain

$$
\begin{aligned}
&\frac{\mathrm{d}p_2}{\mathrm{d}\tau}\,\mathrm{D}_1 f_2(M_1,M_2) + p_2\left(\mathrm{D}_{11} f_2(M_1,M_2)\,\frac{\mathrm{d}M_1}{\mathrm{d}\tau} + \mathrm{D}_{12} f_2(M_1,M_2)\,\frac{\mathrm{d}M_2}{\mathrm{d}\tau}\right)\\
&\quad - \mu\, e^{-\mu\,(T-\tau)}\,(\mathrm{D}_1 f_1(M_1,M_2) - g'(M_1) - \mu)\\
&\quad - e^{-\mu\,(T-\tau)}\left((\mathrm{D}_{11} f_1(M_1,M_2) - g''(M_1))\,\frac{\mathrm{d}M_1}{\mathrm{d}\tau} + \mathrm{D}_{12} f_1(M_1,M_2)\,\frac{\mathrm{d}M_2}{\mathrm{d}\tau}\right) = 0,\\
&\Big(p_2\,(\mathrm{D}_2 f_2(M_1,M_2) - g'(M_2)) - e^{-\mu\,(T-\tau)}\,\mathrm{D}_2 f_1(M_1,M_2)\Big)\cdot \mathrm{D}_1 f_2(M_1,M_2)\\
&\quad + p_2\left(\mathrm{D}_{11} f_2(M_1,M_2)\,\frac{\mathrm{d}M_1}{\mathrm{d}\tau} + \mathrm{D}_{12} f_2(M_1,M_2)\,\frac{\mathrm{d}M_2}{\mathrm{d}\tau}\right)\\
&\quad - \mu\, e^{-\mu\,(T-\tau)}\,(\mathrm{D}_1 f_1(M_1,M_2) - g'(M_1) - \mu)\\
&\quad - e^{-\mu\,(T-\tau)}\left((\mathrm{D}_{11} f_1(M_1,M_2) - g''(M_1))\,\frac{\mathrm{d}M_1}{\mathrm{d}\tau} + \mathrm{D}_{12} f_1(M_1,M_2)\,\frac{\mathrm{d}M_2}{\mathrm{d}\tau}\right) = 0,
\end{aligned}
$$

and, after substituting (56) and canceling $e^{-\mu\,(T-\tau)}$,

$$
\begin{aligned}
&\frac{\mathrm{d}M_1}{\mathrm{d}\tau}\left(\frac{\mathrm{D}_{11} f_2(M_1,M_2)\,(\mathrm{D}_1 f_1(M_1,M_2) - g'(M_1) - \mu)}{\mathrm{D}_1 f_2(M_1,M_2)}\right.\\
&\quad \left. - \mathrm{D}_{11} f_1(M_1,M_2) + g''(M_1)\right)\\
&\quad + \frac{\mathrm{d}M_2}{\mathrm{d}\tau}\left(\frac{\mathrm{D}_{12} f_2(M_1,M_2)\,(\mathrm{D}_1 f_1(M_1,M_2) - g'(M_1) - \mu)}{\mathrm{D}_1 f_2(M_1,M_2)} - \mathrm{D}_{12} f_1(M_1,M_2)\right)\\
&\quad - \mathrm{D}_2 f_1(M_1,M_2)\,\mathrm{D}_1 f_2(M_1,M_2)\\
&\quad + (\mathrm{D}_1 f_1(M_1,M_2) - g'(M_1) - \mu)\,(\mathrm{D}_2 f_2(M_1,M_2) - g'(M_2) - \mu) = 0,
\end{aligned}
\tag{57}
$$

$$
\begin{aligned}
&(1-u_1)\,f_1(M_1,M_2) - g(M_1)\\
&\quad = \left(\frac{\mathrm{D}_{11} f_2(M_1,M_2)\,(\mathrm{D}_1 f_1(M_1,M_2) - g'(M_1) - \mu)}{\mathrm{D}_1 f_2(M_1,M_2)}\right.\\
&\qquad \left. - \mathrm{D}_{11} f_1(M_1,M_2) + g''(M_1)\right)^{-1}\cdot\,((g(M_2) - f_2(M_1,M_2))\\
&\qquad \cdot\left(\frac{\mathrm{D}_{12} f_2(M_1,M_2)\,(\mathrm{D}_1 f_1(M_1,M_2) - g'(M_1) - \mu)}{\mathrm{D}_1 f_2(M_1,M_2)} - \mathrm{D}_{12} f_1(M_1,M_2)\right)\\
&\qquad - \mathrm{D}_2 f_1(M_1,M_2)\,\mathrm{D}_1 f_2(M_1,M_2)\\
&\qquad + (\mathrm{D}_1 f_1(M_1,M_2) - g'(M_1) - \mu)\,(\mathrm{D}_2 f_2(M_1,M_2) - g'(M_2) - \mu)\Big).
\end{aligned}
$$

Regime 4 Similarly to the reasonings for regime 3, we consecutively derive

$$
\mathrm{D}_2 f_2(M_1,M_2) - g'(M_2) - \mu = 0, \tag{58}
$$

$$
\begin{aligned}
&(\mathrm{D}_{22} f_2(M_1,M_2) - g''(M_2))\,(g(M_2) - (1-u_2)\,f_2(M_1,M_2))\\
&\quad + \mathrm{D}_{12} f_2(M_1,M_2)\,(g(M_1) - f_1(M_1,M_2)) = 0,
\end{aligned}
\tag{59}
$$

$$
(1-u_2)\,f_2(M_1,M_2) - g(M_2) = \frac{\mathrm{D}_{12} f_2(M_1,M_2)\,(g(M_1) - f_1(M_1,M_2))}{\mathrm{D}_{22} f_2(M_1,M_2) - g''(M_2)}
$$

in the degenerate case $n_2 = 0$, and

$$
\begin{aligned}
&\frac{\mathrm{d}M_2}{\mathrm{d}\tau}\left(\frac{\mathrm{D}_{22}f_1(M_1,M_2)\,(\mathrm{D}_2f_2(M_1,M_2)-g'(M_2)-\mu)}{\mathrm{D}_2f_1(M_1,M_2)}\right.\\
&\quad\left.-\,\mathrm{D}_{22}f_2(M_1,M_2)+g''(M_2)\right)\\
&\quad+\;\frac{\mathrm{d}M_1}{\mathrm{d}\tau}\left(\frac{\mathrm{D}_{12}f_1(M_1,M_2)\,(\mathrm{D}_2f_2(M_1,M_2)-g'(M_2)-\mu)}{\mathrm{D}_2f_1(M_1,M_2)}-\mathrm{D}_{12}f_2(M_1,M_2)\right)\\
&\quad-\;\mathrm{D}_1f_2(M_1,M_2)\,\mathrm{D}_2f_1(M_1,M_2)\\
&\quad+\;(\mathrm{D}_2f_2(M_1,M_2)-g'(M_2)-\mu)\,(\mathrm{D}_1f_1(M_1,M_2)-g'(M_1)-\mu)=0,
\end{aligned}
\tag{60}
$$

$$
\begin{aligned}
&(1-u_2)\,f_2(M_1,M_2)-g(M_2)\\
&\quad=\;\left(\frac{\mathrm{D}_{22}f_1(M_1,M_2)\,(\mathrm{D}_2f_2(M_1,M_2)-g'(M_2)-\mu)}{\mathrm{D}_2f_1(M_1,M_2)}\right.\\
&\qquad\left.-\,\mathrm{D}_{22}f_2(M_1,M_2)+g''(M_2)\right)^{-1}\cdot\,((g(M_1)-f_1(M_1,M_2))\\
&\qquad\cdot\left(\frac{\mathrm{D}_{12}f_1(M_1,M_2)\,(\mathrm{D}_2f_2(M_1,M_2)-g'(M_2)-\mu)}{\mathrm{D}_2f_1(M_1,M_2)}-\mathrm{D}_{12}f_2(M_1,M_2)\right)\\
&\qquad-\;\mathrm{D}_1f_2(M_1,M_2)\,\mathrm{D}_2f_1(M_1,M_2)\\
&\qquad+\;(\mathrm{D}_2f_2(M_1,M_2)-g'(M_2)-\mu)\,(\mathrm{D}_1f_1(M_1,M_2)-g'(M_1)-\mu)\big)
\end{aligned}
$$

if $\mathrm{D}_2f_1(M_1,M_2)\neq 0$ on the considered subarc.

3.3.2.2 *Stationary feedback control law*

The next theoretical constructions are needed in order to describe the stationary feedback control law for such parts of the reverse-time characteristics that emanate from the positions (48) (and then either leave the plane $M_1=M_2$ at some $\tau\in[\tau',T)$ or stay there till $\tau=T$).

Consider the four reverse-time dynamical systems that are obtained from (26) by substituting the feedback control pairs for the studied regimes 1–4. Let us refer to them as systems 1–4, respectively.

A number of additional assumptions have to be adopted.

Assumption 3.12 For every $j\in\{1,2,3,4\}$, there exists a closed domain $\bar{D}_j\subseteq\bar{G}$ such that $(M^{**},M^{**})\in D_j\overset{\text{def}}{=}\operatorname{int}\bar{D}_j$ and the right-hand side of the system j is defined and continuously differentiable in $\bar{D}_j$.

For convenience, let $\tau=0$ be the initial instant for systems 1–4 (since they are autonomous, one can choose an arbitrary initial instant for them, not necessarily $\tau\geqslant\tau^{**}$), and set the initial condition as $(M_1,M_2)|_{\tau=0}=(M^{**},M^{**})$. For every $j\in\{1,2,3,4\}$, consider the resulting Cauchy problem for the system j on the maximum extendability interval $[0,\theta_j)$ until the first exit from the open domain D_j (the case $\theta_j<+\infty$) or up to infinity (the case $\theta_j=+\infty$) if there is no such an exit. Denote the related state trajectories by Σ_1–Σ_4, respectively. Here we do not restrain the time intervals by the number $T-\tau^{**}$, because we want to make our constructions independent from a particular finite time horizon T.

The following assumption means that the singular control components for regimes 1–4 correspond to intermediate configurations of resource allocation. (This is rather typical for singular policies, while bang–bang policies take only boundary values.)

Assumption 3.13 For every $j\in\{1,2,3,4\}$, the singular control component for the regime j lies in $(0,1)$ on the state trajectory Σ_j.

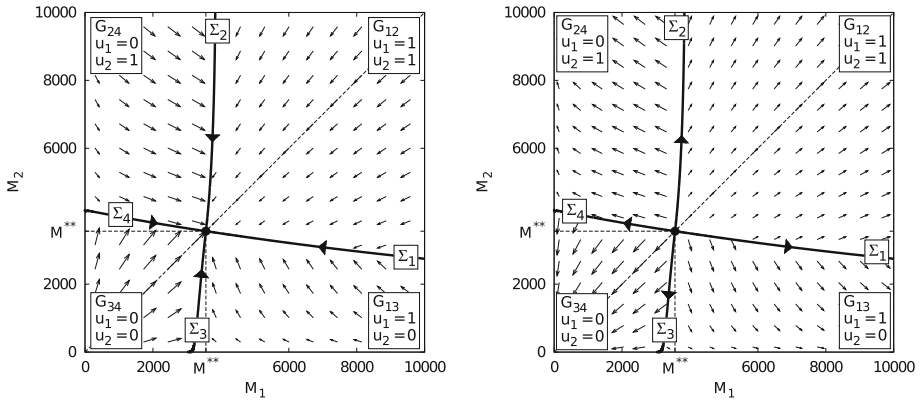

(a) Forward-time velocities **(b)** Reverse-time velocities

Fig. 3 The feedback control law (61) for the functions (5)–(7) and parameter values (10). The velocities are drawn (**a**) in forward time and (**b**) in reverse time

In Sect. B.2.1 of Online Appendix B, the following properties of the curves Σ_1–Σ_4 are established under Assumptions 2.1–2.4, 3.3, 3.5, 3.8, 3.10, 3.12, 3.13 (for better understanding, it is useful to look at Fig. 3 in advance, that figure is related to the functions (5)–(7) and parameter values (10)):

– the state trajectories Σ_1–Σ_4 are regular curves located so that

$$(\Sigma_1 \cup \Sigma_3) \setminus \{(M^{**}, M^{**})\} \subset \{(M_1, M_2) \in G : M_1 > M_2\},$$
$$(\Sigma_2 \cup \Sigma_4) \setminus \{(M^{**}, M^{**})\} \subset \{(M_1, M_2) \in G : M_1 < M_2\};$$

– the time bounds θ_1, θ_2 for the state trajectories Σ_1, Σ_2 are finite (however, general analytical verification of whether the time bounds θ_3, θ_4 for the state trajectories Σ_3, Σ_4 are finite or infinite remains an open problem);
– if $j \in \{1, 2, 3, 4\}$ and $\theta_j < +\infty$, then the limit endpoint of Σ_j for $\tau \nearrow \theta_j$ lies neither on the line $M_1 = 0$ nor on the line $M_2 = 0$;
– if $j \in \{1, 3\}$, then the limit endpoint of Σ_j for $\tau \nearrow \theta_j$ belongs to the closed half-plane $M_1 \geqslant M_2$;
– if $j \in \{2, 4\}$, then the limit endpoint of Σ_j for $\tau \nearrow \theta_j$ belongs to the closed half-plane $M_1 \leqslant M_2$.

In line with the next assumption, all curves Σ_1–Σ_4 end on the boundary of G.

Assumption 3.14 For every $j \in \{1, 2, 3, 4\}$, the limit endpoint of the state trajectory Σ_j for $\tau \nearrow \theta_j$ lies on the boundary ∂G of the domain (2).

For describing the sought-after feedback control law, the following assumption plays a crucial role. In particular, it guarantees that the reverse-time characteristics do not have any switchings after exiting from the singular control regimes on the curves Σ_1–Σ_4. This can be verified with the help of the same representations for the first and second derivatives of the switching functions $e^{-\mu(T-\tau)} + p_1$, $e^{-\mu(T-\tau)} - p_2$ and related expressions as were used in the above analysis of regimes 1–4.

Assumption 3.15 The following conditions hold (see Fig. 3b):

(1) the sets $\Sigma_j \setminus \{(M^{**}, M^{**})\}$, $j = \overline{1,4}$, are mutually disjoint (which implies that the only common point of Σ_1–Σ_4 is (M^{**}, M^{**}));
(2) the curves Σ_1–Σ_4 divide the strongly invariant region G into four open domains $G_{12}, G_{13}, G_{24}, G_{34}$, so that

$$G = \left(\bigcup_{j=1}^{4} \Sigma_j \right) \cup G_{12} \cup G_{13} \cup G_{24} \cup G_{34}$$

and, for $(j_1, j_2) = (1,2), (1,3), (2,4), (3,4)$, the domain $G_{j_1 j_2}$ is located between the curves Σ_{j_1} and Σ_{j_2}, i.e.,

$$\Sigma_{j_1} \cup \Sigma_{j_2} \subseteq \partial G_{j_1 j_2} \subseteq \Sigma_{j_1} \cup \Sigma_{j_2} \cup \partial G;$$

(3) on $\Sigma_1 \cup \Sigma_2$, the vector of the right-hand side of the reverse-time system (26) with $(u_1, u_2) = (1,1)$ is directed strictly inside the domain G_{12};
(4) on $\Sigma_1 \cup \Sigma_3$, the vector of the right-hand side of the reverse-time system (26) with $(u_1, u_2) = (1,0)$ is directed strictly inside the domain G_{13};
(5) on $\Sigma_2 \cup \Sigma_4$, the vector of the right-hand side of the reverse-time system (26) with $(u_1, u_2) = (0,1)$ is directed strictly inside the domain G_{24};
(6) on $\Sigma_3 \cup \Sigma_4$, the vector of the right-hand side of the reverse-time system (26) with $(u_1, u_2) = (0,0)$ is directed strictly inside the domain G_{34};
(7) the left-hand side of (49) is negative in $G_{12} \cup (\Sigma_2 \setminus \{(M^{**}, M^{**})\})$ and positive in $G_{13} \cup (\Sigma_3 \setminus \{(M^{**}, M^{**})\})$, the coefficient near u_2 in (50) is negative on Σ_1 (note that, under Assumption 3.5, negativity of this coefficient is equivalent to negativity of $\mathrm{D}_{22}[f_2 - f_1](M_1, M_2)$);
(8) the left-hand side of (51) is negative in $G_{12} \cup (\Sigma_1 \setminus \{(M^{**}, M^{**})\})$ and positive in $G_{24} \cup (\Sigma_4 \setminus \{(M^{**}, M^{**})\})$, the coefficient near u_1 in (52) is negative on Σ_2 (note that, under Assumption 3.5, negativity of this coefficient is equivalent to negativity of $\mathrm{D}_{11}[f_1 - f_2](M_1, M_2)$);
(9) in the degenerate case $n_1 = 0$, the left-hand side of (54) is negative in G_{13} and positive in G_{34}, and the coefficient near u_1 in (55) is negative on Σ_3 (note that, under Assumption 3.5, negativity of this coefficient is equivalent to negativity of $\mathrm{D}_{11} f_1(M_1, M_2)$);
(10) if $n_1 > 0$, then the left-hand side of (57) with $(dM_1/d\tau, dM_2/d\tau)$ determined by (26) with $(u_1, u_2) = (1,0)$ is positive in $\Sigma_1 \cup \Sigma_3 \cup G_{13}$, and, for $(u_1, u_2) = (0,0)$, this expression is negative in $\Sigma_3 \cup \Sigma_4 \cup G_{34}$;
(11) in the degenerate case $n_2 = 0$, the left-hand side of (58) is negative in G_{24} and positive in G_{34}, and the coefficient near u_2 in (59) is negative on Σ_4 (note that, under Assumption 3.5, negativity of this coefficient is equivalent to negativity of $\mathrm{D}_{22} f_2(M_1, M_2)$);
(12) if $n_2 > 0$, then the left-hand side of (60) with $(dM_1/d\tau, dM_2/d\tau)$ determined by (26) with $(u_1, u_2) = (0,1)$ is positive in $\Sigma_2 \cup \Sigma_4 \cup G_{24}$, and, for $(u_1, u_2) = (0,0)$, this expression is negative in $\Sigma_3 \cup \Sigma_4 \cup G_{34}$.

Remark 3.16 If a rigorous analytical verification of Assumptions 3.12–3.15 turns out to be very difficult, it is reasonable to check them informally, based on numerical approximations of the state trajectories Σ_1–Σ_4 (one-dimensional curvilinear grids) and domains $G_{12}, G_{13}, G_{24}, G_{34}$ (two-dimensional grids). This has been done in the particular case of the functions (5)–(7) and parameter values (10), when obtaining the numerical results for Fig. 3. □

By using the above characterizations of the singular control regimes 1–4 and related state trajectories Σ_1–Σ_4 (dividing G into the subdomains G_{12}, G_{13}, G_{24}, G_{34}), we directly arrive at the main result of this subsection (see also Fig. 3).

Theorem 3.17 *Suppose that $T < +\infty$ and Assumptions 2.1–2.4, 3.3, 3.5, 3.8, 3.10, 3.12–3.15 hold. The following representation describes the feedback control law for such parts of the reverse-time characteristics of (26)–(29) that emanate from the positions (48):*

$$(u_1(M_1, M_2),\ u_2(M_1, M_2)) = \begin{cases} (1,1), & (M_1, M_2) \in G_{12}, \\ (1,0), & (M_1, M_2) \in G_{13}, \\ (0,1), & (M_1, M_2) \in G_{24}, \\ (0,0), & (M_1, M_2) \in G_{34}. \end{cases}$$

Furthermore, the regime $u_1 = u_2 = u^{**}$ should be applied for staying at $M_1 = M_2 = M^{**}$, and regimes 1–4 should be used for staying on $\Sigma_j \setminus \{(M^{**}, M^{**})\}$, $j = \overline{1,4}$, respectively. When considering the characteristics in forward time, this feedback map becomes single-valued everywhere in G and takes the form

$$\begin{aligned} &(u_1(M_1, M_2),\ u_2(M_1, M_2)) \\ &\quad = \begin{cases} (1,1), & (M_1, M_2) \in G_{12}, \\ (1,0), & (M_1, M_2) \in G_{13}, \\ (0,1), & (M_1, M_2) \in G_{24}, \\ (0,0), & (M_1, M_2) \in G_{34}, \\ (u^{**}, u^{**}), & M_1 = M_2 = M^{**}, \\ \text{as in the regime } j, & (M_1, M_2) \in \Sigma_j \setminus \{(M^{**}, M^{**})\}, \quad j = \overline{1,4}. \end{cases} \end{aligned} \tag{61}$$

Figure 3 illustrates numerical approximations of the state trajectories Σ_1–Σ_4 and feedback control law (61) for the functions (5)–(7) and parameter values (10). We take $\bar{M}_1 = \bar{M}_2 = \bar{M}$ as in Example 2.8. In the case (5)–(7), (10), we choose this bound as $\bar{M} = 3.5 \cdot 10^4 > \hat{M} \approx 3.167 \cdot 10^4$, which is much greater than $M^{**} \approx 0.356 \cdot 10^4$. In order to focus on the key aspects of the feedback map in a neighborhood of the point (M^{**}, M^{**}), we show the portrait only on a subdomain of G. The portrait on the remaining part of G is clear, and, in particular, the state trajectories Σ_1 and Σ_2 end on the lines $M_1 = \bar{M}$ and $M_2 = \bar{M}$, respectively. On the lines $M_2 = 0$ and $M_1 = 0$, one can see the limit endpoints of Σ_3 and Σ_4, respectively. The fields of the forward-time and reverse-time velocities (i.e., the vectors of the right-hand sides of the dynamical systems (22) and (26) with the substituted control law (61)) are also indicated in the two subfigures. The point (M^{**}, M^{**}) appears to be an attractor for the considered parts of the forward-time characteristics.

Remark 3.18 In Sect. B.2.2 of Online Appendix B, it is proved that, under the conditions of Theorem 3.17, the singular feedback strategies u_2 in the regimes 1,4 and u_1 in the regimes 2,3 continuously join the value u^{**} at the state (M^{**}, M^{**}) only if $n_1 = n_2$ or $\nu'((n_1 + n_2)\, M^{**}) = 0$ (which is a rather narrow case). □

Let the conditions of Theorem 3.17 hold. Then the curves $\Sigma_i \setminus \{(M^{**}, M^{**})\}$, $i = \overline{1,4}$, are universal manifolds, and there is no kind of "perpetuated dilemma", contrary to equivocal manifolds [6,28,34]. Indeed, upon reaching any of these curves from the domain G_{12}, G_{13}, G_{24} or G_{34}, one cohort has to switch its control from 0 or 1 to the appropriate singular regime, while the other one keeps its control 0 or 1. The situation with entering the doubly

singular regime $u_1 = u_2 = u^{**}$ at the state (M^{**}, M^{**}) (from any of the curves $\Sigma_i \setminus \{(M^{**}, M^{**})\}$, $i = \overline{1,4}$, or directly from $G_{13} \cup G_{24}$) is much more complicated. In fact, these are junctions with a one-dimensional curve in a three-dimensional space (one has two state variables and a time variable), i.e., junctions with a manifold of codimension 2. To our knowledge, a clear theory of such junctions is currently missing. The best hint we have for the correctness of our analytical constructions is a very good agreement with the switching surfaces obtained from a numerical solution of the Cauchy problem for the HJI equation (see Fig. 6 in Sect. 4).

3.4 Resulting Conjecture on the Structure of the Saddle State-Feedback Control Strategies in the Infinite-Horizon Case

For drawing rigorous conclusions about the structure of the saddle state-feedback control strategies in case $T < +\infty$, the global portrait of the characteristics of the problem (19) has to be described. But, as opposed to the characteristics with $M_1|_{\tau=0} = M_2|_{\tau=0}$, complete analytical investigation of the field of the characteristics with $M_1|_{\tau=0} \neq M_2|_{\tau=0}$ appears to be very difficult. In the coordinate space (M_1, M_2, τ) with the vertical axis τ, the latter are located below the characteristic arcs emanating from the positions (48). According to Theorem 3.6, the regions $M_1 > M_2$ and $M_1 < M_2$ are invariant for the reverse-time characteristics. Furthermore, Remark 3.7 specifies the order in which the characteristics with $M_1|_{\tau=0} \neq M_2|_{\tau=0}$ may reach the corresponding switching surfaces. One can expect that there should be four such surfaces (two in each of the domains $M_1 > M_2$ and $M_1 < M_2$) and they continuously join the other switching surfaces generated by the singular control regimes 1–4 from Sect. 3.3.2. Even though this property has not been proved in our characteristic analysis, the numerical simulation results of the next section will give the related informal verification (see Fig. 7). It is also natural to observe that the reduction in the saddle state-feedback control map to the horizontal plane for a fixed time instant is determined by four domains and four separating curves, and, for sufficiently large T and $\tau \stackrel{\text{def}}{=} T - t$, the latter differ from Σ_1–Σ_4 only near the boundary ∂G (see Fig. 6). More precisely, this difference is likely to tend to zero as $\tau \to +\infty$, and there should even be exact coincidence with Σ_1 for $\tau \geqslant \tau^{**} + \theta_1$ and with Σ_2 for $\tau \geqslant \tau^{**} + \theta_2$. (Finiteness of the time bounds θ_1, θ_2 is one of the properties mentioned directly after Assumption 3.13.)

Thus, we arrive at the conjecture that, in the infinite-horizon case $T = +\infty$, the saddle state-feedback control strategies should have the same stationary form (61) as given in Theorem 3.17 for the characteristic arcs emanating from the positions (48). A rigorous proof of this statement remains an open problem. The next section will contain some justification based on the results of numerical simulations for a sufficiently large finite horizon T.

Conjecture 3.19 *Under Assumptions* 2.1–2.4, 3.3, 3.5, 3.8, 3.10, 3.12–3.15, *the saddle state-feedback control map for the differential game* (13)–(15) *in case* $T = +\infty$ *takes the form* (61).

In the related characteristic portrait (see Fig. 3a), one can see the attractor (M^{**}, M^{**}), which is reached in finite time either through the diagonal $M_1 = M_2$ (invariant in forward time), or from the domains G_{13}, G_{24}, or through one of the turnpike curves Σ_1–Σ_4. After entering the attractor, the forward-time characteristics stay there indefinitely.

4 Finite-Difference Approximation

We have used the software ROC-HJ [11] in order to approximate the viscosity solution of the problem (19) (i.e., the value function $V_{\text{VREK}} = V_{\text{s-f}} = V$ of the differential game (13)–(15) in nonanticipative or state-feedback strategies) for the time horizon $T = 60$, functions (5)–(7), and parameter values (10) by the method of finite differences [12,15,23,39]. For numerical purposes, it is convenient to rewrite (19) in reverse time $\tau \stackrel{\text{def}}{=} T - t$ as

$$\begin{cases} \dfrac{\partial V(T-\tau, M_1, M_2)}{\partial \tau} + \max_{u_1 \in [0,1]} \min_{u_2 \in [0,1]} \left(-H\left(T-\tau,\ M_1,\ M_2,\ u_1,\ u_2,\right.\right. \\ \qquad \left.\left. \dfrac{\partial V(T-\tau, M_1, M_2)}{\partial M_1},\ \dfrac{\partial V(T-\tau, M_1, M_2)}{\partial M_2}\right)\right) = 0, \\ V(T-\tau, M_1, M_2)\,|_{\tau=0} = 0, \\ \tau \in [0, T], \quad (M_1, M_2) \in G, \end{cases} \tag{62}$$

and then to rewrite (62) in the new state variables

$$m_i \stackrel{\text{def}}{=} M_i \cdot 10^{-4}, \quad i = 1, 2$$

(Such changes in the time and state variables will lead to equivalent approximation results.) Let us take $\bar{M}_1 = \bar{M}_2 = \bar{M} = 3.5 \cdot 10^4$, $\bar{m} \stackrel{\text{def}}{=} \bar{M} \cdot 10^{-4} = 3.5$ and discretize the computational region

$$\{(m_1, m_2, \tau) :\ 0 \leqslant m_1 \leqslant \bar{m},\ \ 0 \leqslant m_2 \leqslant \bar{m},\ \ 0 \leqslant \tau \leqslant T\}$$

by the spatial step $\Delta m_1 = \Delta m_2 = \Delta m = 2 \cdot 10^{-3}$ and time step $\Delta \tau = 5 \cdot 10^{-3}$. For achieving faster practical convergence, it is reasonable to apply the second-order ENO scheme (for approximating the partial derivatives with respect to the state variables) coupled with the second-order Runge–Kutta time discretization scheme [11,39]. In fact, we have also tested the classical first-order monotone Lax–Friedrichs scheme [11,15,39] (which ensures a theoretical convergence property and an error estimate), and it has given similar results, but with slower actual convergence.

After obtaining the value function V, an efficient practical way of constructing the saddle state-feedback control strategies outside the switching sets is to use the representations (21) with numerical approximations of the partial derivatives $\partial V / \partial M_i$, $i = 1, 2$, although this is not completely rigorous if the gradient of V has discontinuities. Note that, due to the general properties of value functions for zero-sum closed-loop differential games [12,53] and boundedness of the strongly invariant domain G, the value function V for our problem is Lipschitz continuous in $[0, T] \times G$, and, by Rademacher's theorem, it is differentiable almost everywhere in $(0, T) \times G$ (except possibly a subset of Lebesgue measure zero). In order to compute the values of the partial derivatives $\partial V / \partial M_i$, $i = 1, 2$, we have used the standard second-order symmetrized approximation [44, Sect. 5.7].

Figures 4 and 5 illustrate the reductions in the approximate value function and corresponding saddle state-feedback control strategies to the coordinate plane (m_1, m_2) for different time instants. As in Fig. 3, the portraits are depicted on relevant subregions of the strongly invariant domain G. Figure 5 also shows the fields of the related forward-time velocities.

The reductions in the value function in Fig. 4 seem to be continuously differentiable. Moreover, they vanish on the diagonal $m_1 = m_2$ (invariant for the forward-time characteristics), which leads to the conjecture that the two cohorts should have equal saddle state-feedback control strategies there. This also conforms with Fig. 3. Besides, if $M_1^0 = M_2^0$, then one can

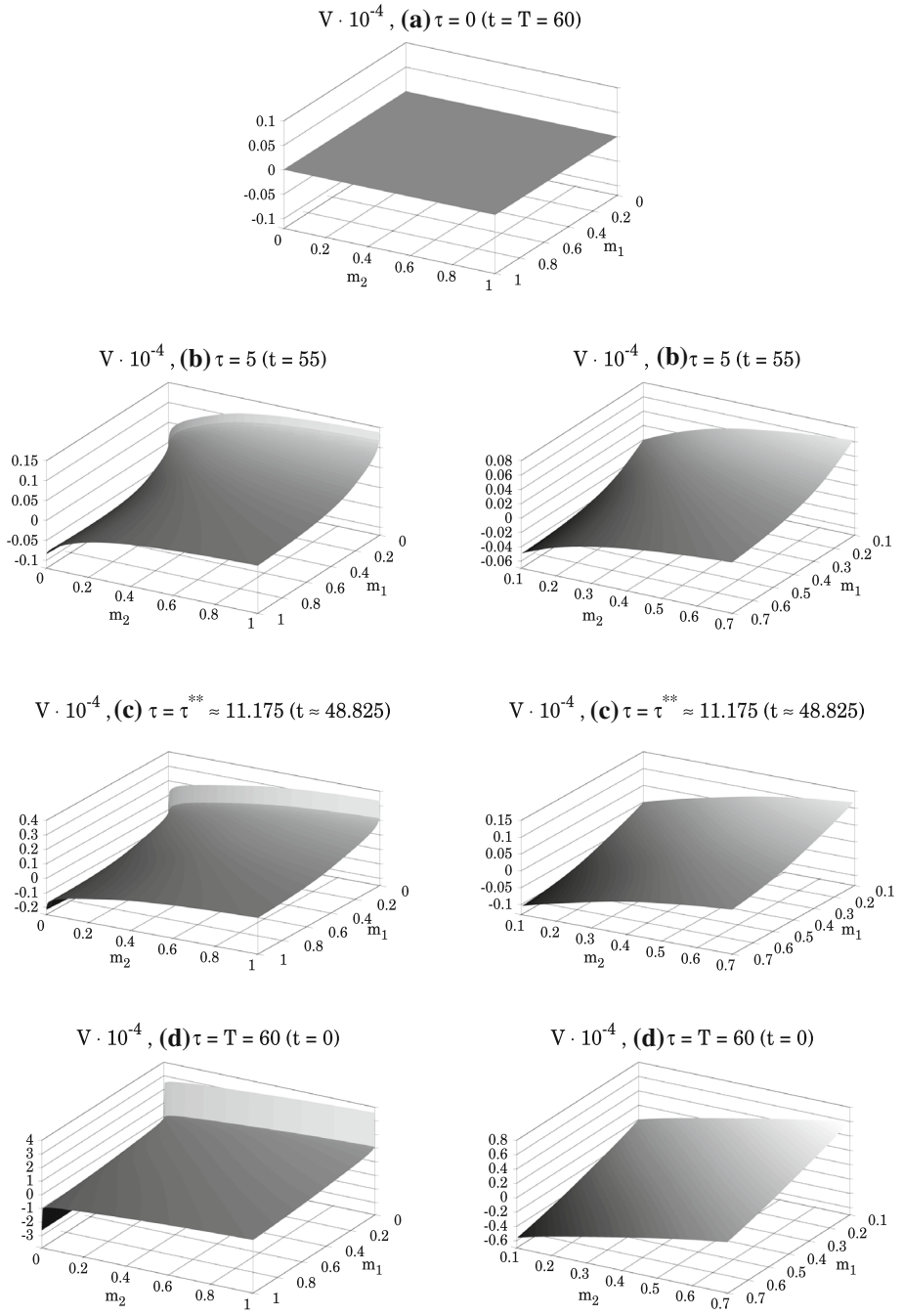

Fig. 4 The finite-difference approximation of the value function V of the differential game (13)–(15) (in the nonanticipative or state-feedback sense) for the time horizon $T = 60$, functions (5)–(7), and parameter values (10). The subfigures illustrate the reductions to the domains $(0, 1)^2$ and $(0.1, 0.7)^2$ on the coordinate plane (m_1, m_2) for the time instants (**a**) $\tau = 0$ ($t = T = 60$), (**b**) $\tau = 5$ ($t = T - 5 = 55$), (**c**) $\tau = \tau^{**} \approx 11.175$ ($t = T - \tau^{**} \approx 48.825$), (**d**) $\tau = T = 60$ ($t = 0$). In order to see the graphs clearer, we do not fix the same scale for the vertical axes in the subfigures

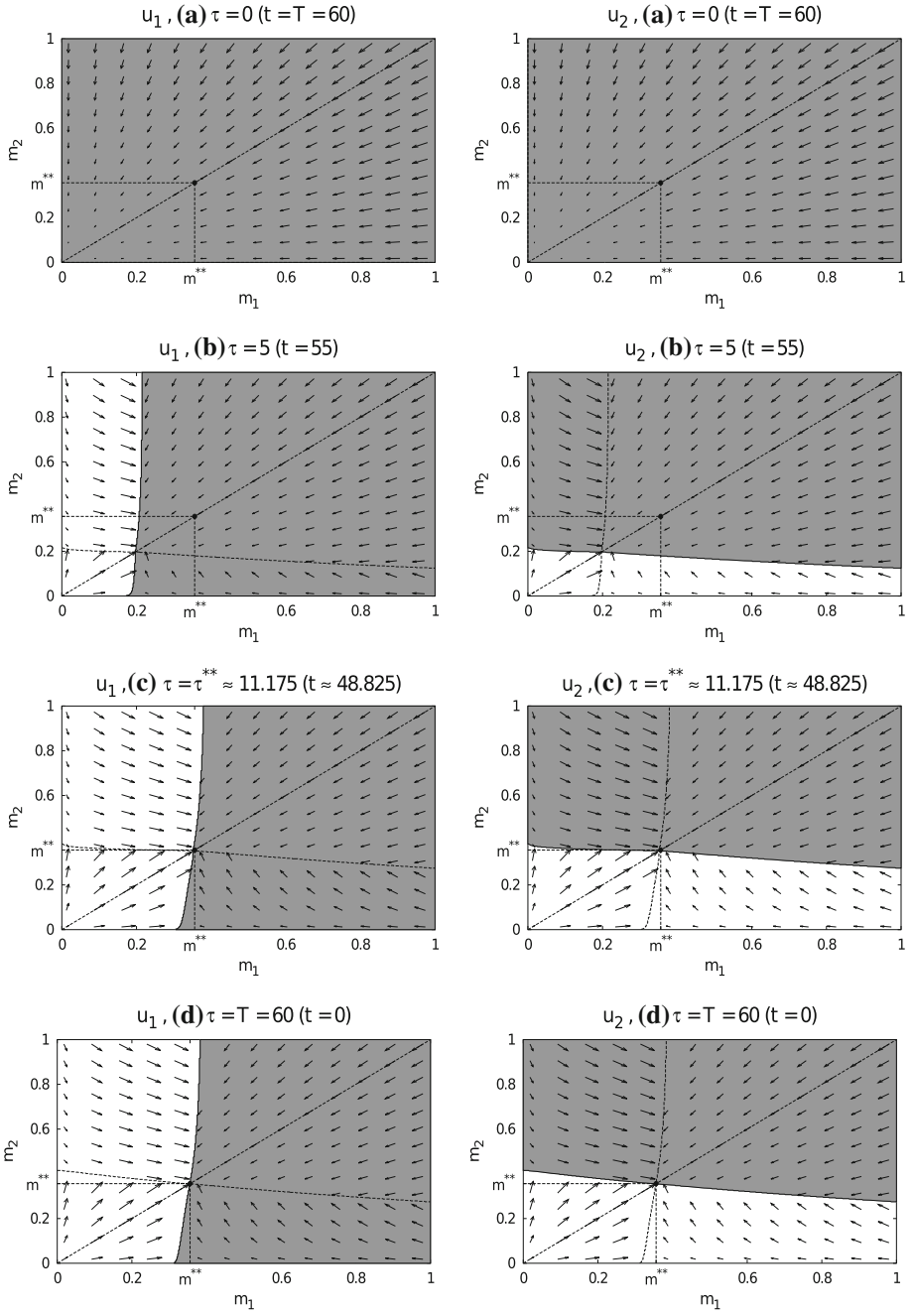

Fig. 5 The finite-difference approximations of the saddle state-feedback control strategies in the differential game (13)–(15) for the time horizon $T = 60$, functions (5)–(7), and parameter values (10). The subfigures illustrate the reductions to the domain $(0, 1)^2$ on the coordinate plane (m_1, m_2) for the time instants (**a**) $\tau = 0$ $(t = T = 60)$, (**b**) $\tau = 5$ $(t = T - 5 = 55)$, (**c**) $\tau = \tau^{**} \approx 11.175$ $(t = T - \tau^{**} \approx 48.825)$, (**d**) $\tau = T = 60$ $(t = 0)$. White and gray colors indicate regions of the control values 0 and 1, respectively. The fields of the related forward-time velocities are also shown

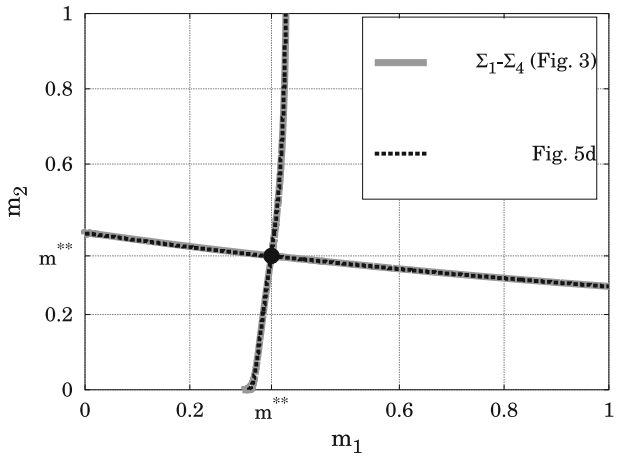

Fig. 6 Comparison of the curves $\Sigma_1 - \Sigma_4$ from Fig. 3 with the four approximate switching curves from Fig. 5d

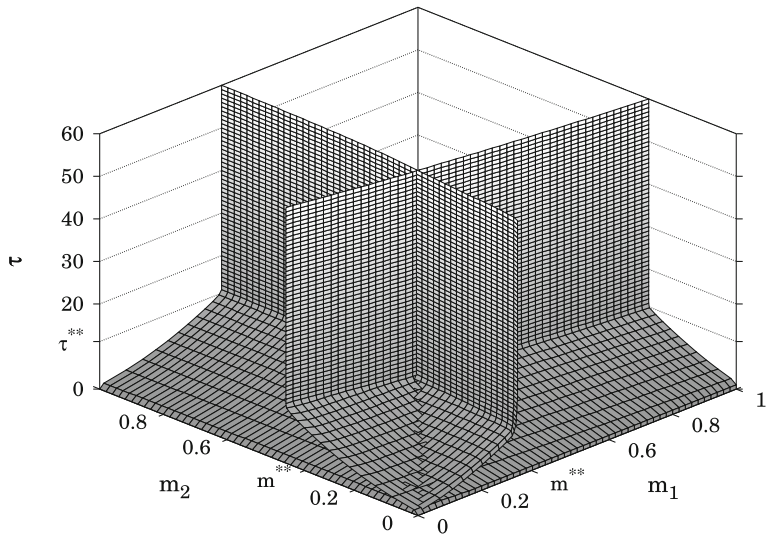

Fig. 7 The four approximate switching surfaces in the coordinate space (m_1, m_2, τ) for the closed-loop differential game (13)–(15) with the time horizon $T = 60$, functions (5)–(7), and parameter values (10)

expect equality of the components in the resulting open-loop control pairs that arise from the definitions of nonanticipative strategies of the cohorts.

Figure 5 indicates the appearance and time evolution of four approximate switching curves. For $\tau \geqslant \tau^{**}$, they intersect nearly at the point (m^{**}, m^{**}), where $m^{**} \stackrel{\text{def}}{=} M^{**} \cdot 10^{-4}$. With the further increase in τ, the related feedback control portrait approaches the stationary form (61), as follows from the comparison in Fig. 6. The four resulting switching surfaces in the coordinate space (m_1, m_2, τ) are illustrated in Fig. 7.

Thus, the obtained numerical simulation results can indeed serve as a practical justification for Conjecture 3.19.

From Fig. 5d, we conclude that, in the considered domain of initial states, the value $V\left(0, M_1^0, M_2^0\right)$ of our zero-sum closed-loop differential game is negative for $M_1^0 > M_2^0$, zero for $M_1^0 = M_2^0$, and positive for $M_1^0 < M_2^0$. One can expect this to hold also in the infinite-horizon case (in particular, Conjecture 3.19 yields vanishing of the game value on the diagonal $M_1^0 = M_2^0$). Then, in compliance with the definition of uninvadability given in Sect. 2.2, the obtained saddle state-feedback strategy of cohort 1 is uninvadable if $M_1^0 \geqslant M_2^0$. Similarly, the obtained saddle state-feedback strategy of cohort 2 is uninvadable if $M_1^0 \leqslant M_2^0$.

5 Some Asymptotic Properties in Case of a Large Total Lesion Density

In [56, Section 6], it was shown that, for the optimal control problem (11),(12) under some reasonable conditions, the function

$$X^*(n) \stackrel{\text{def}}{=} n \cdot M^*(n)$$

(describing how the total mycelial size in the singular control regime depends on lesion density) should be strictly increasing, bounded, and therefore saturating on $[0, +\infty)$. This was natural from the biological point of view due to the presence of the competition term $\nu(nM)$ in the model.

For the differential game (13)–(15), the function

$$X^{**}(n) \stackrel{\text{def}}{=} n \cdot M^{**}(n) \tag{63}$$

describes the dependence of the total mycelial (infection) size at the steady state (M^{**}, M^{**}) on the total lesion density $n \stackrel{\text{def}}{=} n_1 + n_2$. Let us establish that (63) also saturates on $[0, +\infty)$ under certain conditions including Assumptions 2.5 and 2.6.

Assumption 2.5 yields that the inequality (38) holds for all $M > 0$ and $n \geqslant 0$. Then, by using item 6 of Assumption 2.4, we conclude that, for any $n \geqslant 0$, the number $M^{**}(n)$ can be defined as a unique positive root of the equation (34) regardless of the bounds for the strongly invariant domain (recall the proof of Theorem 3.1).

Theorem 5.1 *Let Assumptions 2.1, 2.3, 2.6 hold. Also let Assumption 2.4 hold with the modifications mentioned in Assumption 2.5. Then the function (63) is strictly increasing, bounded, and therefore saturating on* $[0, +\infty)$.

Proof Denote

$$\zeta(n, x) \stackrel{\text{def}}{=} \nu(x)\, \rho'\left(\frac{x}{n}\right) - g'\left(\frac{x}{n}\right) - \mu \quad \forall n > 0 \quad \forall x > 0.$$

According to equation (34), we have

$$\zeta\left(n, X^{**}(n)\right) = 0 \quad \forall n > 0. \tag{64}$$

Since $X^{**}(0) = 0$ and $X^{**}(n) > 0$ for all $n > 0$, it suffices to verify positivity of $(X^{**})'(\cdot)$ and boundedness of $X^{**}(\cdot)$ on $(0, +\infty)$.

For all $n > 0$ and $x > 0$, we obtain

$$\begin{aligned} \frac{\partial \zeta(n, x)}{\partial n} &= -\frac{x}{n^2}\left(\nu(x)\, \rho''\left(\frac{x}{n}\right) - g''\left(\frac{x}{n}\right)\right) > 0, \\ \frac{\partial \zeta(n, x)}{\partial x} &= \nu'(x)\, \rho'\left(\frac{x}{n}\right) + \frac{1}{n}\left(\nu(x)\, \rho''\left(\frac{x}{n}\right) - g''\left(\frac{x}{n}\right)\right) < 0. \end{aligned} \tag{65}$$

For every $n > 0$, the pair $(n, X^{**}(n))$ is the value at the point $(n, 0)$ of the inverse to the mapping

$$(0, +\infty) \times (0, +\infty) \ni (n, x) \longrightarrow (n, \zeta(n, x)). \tag{66}$$

The Jacobian of (66) is nonzero for any $n > 0$ and $x > 0$ by virtue of (65). Then, by the classical inverse mapping theorem, $X^{**}(\cdot)$ is continuously differentiable on $(0, +\infty)$, and

$$\frac{\mathrm{d}X^{**}(n)}{\mathrm{d}n} = -\frac{\frac{\partial \zeta\left(n, X^{**}(n)\right)}{\partial n}}{\frac{\partial \zeta(n, X^{**}(n))}{\partial x}} > 0 \quad \forall n > 0.$$

If there exists a sequence $\{n_l\}_{l=1}^{\infty}$ of positive numbers such that $\lim\limits_{l\to\infty} n_l = +\infty$ and $\lim\limits_{l\to\infty} X^{**}(n_l) = +\infty$, then, due to Assumptions 2.5, 2.6, we get

$$\limsup_{l\to\infty} \zeta\left(n_l, X^{**}(n_l)\right) \leqslant -\mu < 0,$$

which contradicts with (64). Thus, $X^{**}(\cdot)$ is bounded on $(0, +\infty)$. □

Remark 5.2 Let Assumptions 2.1, 2.3, 2.6 hold. Also let Assumption 2.4 hold with the following modifications: In its items 1–5, the intervals are extended up to $+\infty$, and, in its item 7, $\tilde{M} \in \left(0, \bar{M}_{\min}\right)$ is replaced with $\tilde{M} > 0$. Moreover, suppose that $n_1 > 0$, $n_2 > 0$, and that $\rho(M) = \alpha M$ and $g(M) = \gamma M$ for all $M \geqslant 0$, where α, γ are positive constants. (All these conditions hold in Example 2.9, while Theorem 5.1 adopts Assumption 2.5 including negativity of $\rho''(\cdot)$ on $(0, +\infty)$.) Then (64) and (65) yield that $\mathrm{d}X^{**}(n)/\mathrm{d}n = 0$ for all $n > 0$, i.e., the total steady-state mycelial size $X^{**}(n)$ does not depend on the total lesion density $n > 0$. By applying similar arguments to equation (36) for the single-cohort optimal control problem, one can derive that $X^*(n)$ does not depend on $n > 0$ under the additional condition that $x\,\nu''(x) + 2\,\nu'(x) \neq 0$ for all $x > 0$ (which also holds in Example 2.9). From the biological point of view, these conclusions seem to be less reasonable than the saturating growth behavior mentioned in Theorem 5.1 and in [56, Section 6]. Indeed, the total infection size is expected to increase with the increase in the total lesion density, at least when the latter is not very large. □

Now let us adopt the representations (5)–(7) with $n \geqslant 0$ and positive constants α, k, β, γ satisfying the inequality (8). Then all the conditions of Theorem 5.1 hold. For numerical simulations, let us also choose the values of all the model parameters except n_1, n_2, n as in (10).

Figure 8 illustrates the graphs of the functions $M^{**}(n)$, $u^{**}(n)$, $X^{**}(n)$ and $u^{**}(n)\,f(M^{**}(n))$. The graphs of the functions $M^*(n)$, $u^*(n)$, $X^*(n)$ and $u^*(n)\,f(M^*(n))$ are also shown for comparison. For positive n in the indicated argument range, the following properties can be seen:

- $M^*(n) < M^{**}(n)$ (in conformity with (37));
- $u^*(n) > u^{**}(n)$, i.e., maintaining the singular control regime for the uninvadable strategies requires lower relative investment in spore production and, consequently, greater relative investment in mycelial growth, compared to the optimal control case;
- $u^*(n)\,f(M^*(n)) > u^{**}(n)\,f(M^{**}(n))$, i.e., the steady-state spore production rate for the uninvadable strategies is smaller than that in the optimal control case;
- as n increases, the functions $M^*(n)$, $M^{**}(n)$, $u^{**}(n)$, $u^*(n)\,f(M^*(n))$ and $u^{**}(n)\,f(M^{**}(n))$ decrease, while $u^*(n)$ stays approximately constant;
- $X^*(n)$ and $X^{**}(n)$ grow and saturate (in agreement with [56, Section 6] and Theorem 5.1).

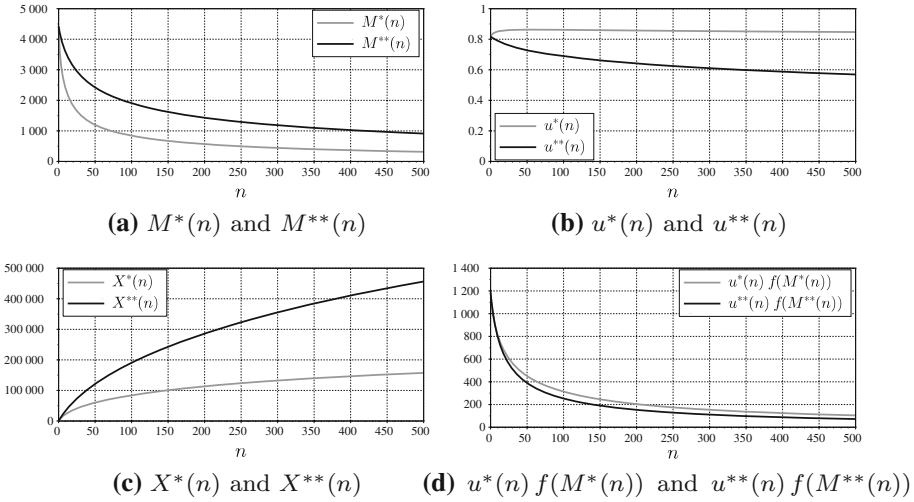

Fig. 8 The graphs of the functions (**a**) $M^{**}(n)$, (**b**) $u^{**}(n)$, (**c**) $X^{**}(n)$, (**d**) $u^{**}(n)\, f(M^{**}(n))$ in case of the representations (5)–(7) and values of all the model parameters except n_1, n_2, n as in (10). The graphs of the functions (**a**) $M^*(n)$, (**b**) $u^*(n)$, (**c**) $X^*(n)$, (**d**) $u^*(n)\, f(M^*(n))$ are also shown for comparison

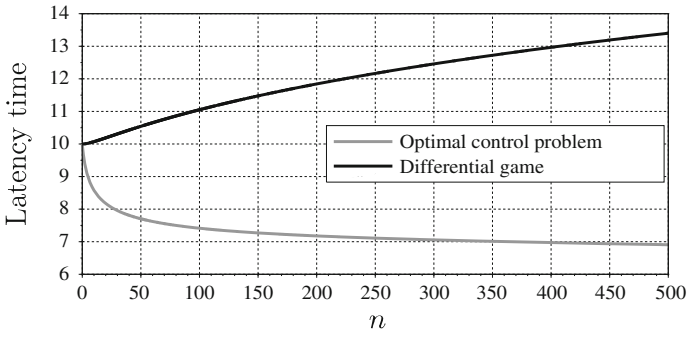

Fig. 9 The dependence of the introduced latency times on n in case of the representations (5)–(7), values of all the model parameters except n_1, n_2, n as in (10), and initial state coordinates $M_1^0 = M_2^0 = 1$

Finally, let us fix $M_1^0 = M_2^0 = 1$ (which means that a mycelium appears from one spore at the beginning of the infection period) and consider the corresponding latency times for the optimal control problem (11),(12) and differential game (13)–(15) in the infinite-horizon case $T = +\infty$. These are the times at which the related forward-time characteristics reach the states $M = M^*$ and $M_1 = M_2 = M^{**}$, respectively (see Theorem A.13 in Online Appendix A and Conjecture 3.19). Let the observed range of positive n be such that $M_1^0 = M_2^0 < M^*(n) < M^{**}(n)$ in it. From the biological point of view, the latency intervals therefore correspond to the time lags with no investment in spore production (zero-control regime).

Figure 9 depicts the dependence of the introduced latency times on n. One can see that, starting already from sufficiently small positive n, the latency time function for the optimal control problem decreases, and the latency time function for the differential game increases. Hence, the influence of the competition term becomes strong enough to significantly slow the

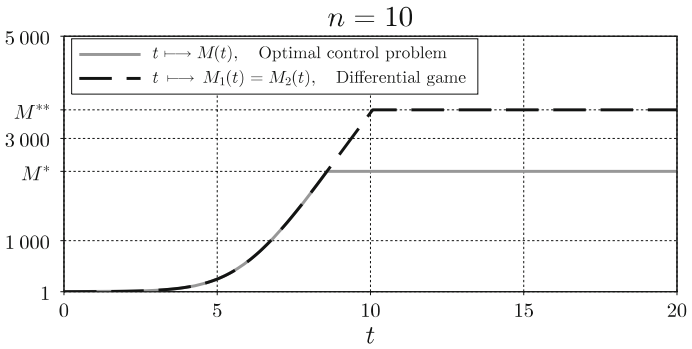

Fig. 10 The trajectories $t \longmapsto M(t)$ (optimal control problem) and $t \longmapsto M_1(t) = M_2(t)$ (differential game) determining the introduced latency times in case of the representations (5)–(7), parameter values (10), and initial state coordinates $M_1^0 = M_2^0 = 1$

mycelial growth when approaching the average size $M^{**}(n)$, while approaching the lower size $M^*(n)$ is not enough for increasing the related latency time with the increase in n. Besides, Fig. 9 indicates tending of the graphs to some horizontal asymptotes. The corresponding trajectories $t \longmapsto M(t)$ (optimal control problem) and $t \longmapsto M_1(t) = M_2(t)$ (differential game) in case of n specified by (10) are shown in Fig. 10. Thus, the game-theoretic competition makes M^{**} greater than M^* at the expense of a delayed onset of spore production.

6 Concluding Remarks

This paper studied a game-theoretic extension of the continuous-time optimal resource allocation problem of [56]. We considered one-seasonal dynamics of two biotrophic fungal cohorts within a common host plant. From the perspective of adaptive dynamics, it was possible to interpret the cohorts as resident and mutant populations. The invasion functional took the form of the difference between the two marginal fitness criteria and represented the cost in the definition of the value of the differential game. The presence of a specific competition term in both equations and marginal fitnesses did not allow us to apply the two-step approach of [10,36,41] relying on optimal control theory. Therefore, the general game-theoretic formulation of [10, Sect. 4.1] with the related concept of uninvadable strategy had to be used. From the mathematical point of view, it was reasonable to consider the class of state-feedback control strategies. The corresponding Cauchy problem for the HJI equation was investigated first analytically by the method of characteristics and then numerically by a finite-difference approximation scheme. The obtained analytical and numerical results turned out to be in good agreement with each other.

The approximated saddle state-feedback strategy of cohort 1 appeared to be uninvadable for $M_1^0 \geqslant M_2^0$, while the related strategy of cohort 2 became uninvadable for $M_1^0 \leqslant M_2^0$ (recall the discussion in the end of Sect. 4).

The curves Σ_1–Σ_4 intersecting at the point $(M_1, M_2) = (M^{**}, M^{**})$ played a crucial role in the analysis of the characteristics of the HJI equation (see Fig. 3). In such a reasonable abstraction as the infinite-horizon case, these were the only switching curves of the saddle state-feedback strategies of the cohorts (according to Conjecture 3.19). The corresponding control law (61) made the forward-time characteristics enter their attractor $(M_1, M_2) = (M^{**}, M^{**})$ (either through the diagonal $M_1 = M_2$, or from the

domains G_{13}, G_{24}, or through the intermediate turnpike regimes on Σ_1–Σ_4) and stay there indefinitely. In the finite-horizon case, additional switching surfaces in the space of the state and time variables appeared, but, for sufficiently large reverse-time instants, the synthesis portrait became almost stationary and very close to the one specified by (61). (The related finite-difference approximation results served as a practical justification for Conjecture 3.19.) It was also verified that, compared to the singular control regime $M = M^*$, $u = u^*$ in the single-cohort optimization problem of [56], maintaining the regime $M_1 = M_2 = M^{**}$, $u_1 = u_2 = u^{**}$ for the uninvadable strategies in the zero-sum differential game would require greater resources (recall Theorem 3.1 and Remark 3.2).

Furthermore, noteworthy asymptotic properties were established. In particular, it was shown that the total infection size at the steady state (M^{**}, M^{**}) should saturate for large total lesion densities. This was reasonable from the biological point of view, because host resources were limited and, when increasing the lesion density, the infections could not infinitely grow. Some numerical experiments were conducted for such a significant pathogen trait as latency time. It also saturated for large total lesion densities, and, in the game-theoretic case, it was greater than in the optimal control case (the game-theoretic competition made M^{**} greater than M^* at the expense of a delayed onset of spore production).

Finally, let us discuss possible future developments of this work. First, the formalism of [6] may help to rigorously prove Conjecture 3.19. Next, long-seasonal dynamics and related evolutionary equilibria of competing biotrophic fungal cohorts are worth investigating. Then specific discrete rules can be adopted in order to model the transition from one season to another [1,31]. Moreover, note that, within the framework of adaptive dynamics, ESS-es can be defined as such equilibria of an appropriately formulated canonical equation (whose type depends on the class of considered traits) that maximize the invasion fitness in the corresponding resident environment [19,20,36,41]. It is important to study not only these equilibria themselves but also whether they indeed represent evolutionary attractors or not, and how they can be approached through evolution. The recent methodology of [20,36,41] for treating function-valued traits cannot be directly applied to our model (mainly because of the competition term). Hence, it is important to extend existing theoretical frameworks for describing evolutionary dynamics of infinite-dimensional traits. Besides, as is noted in Remark 2.10, it is relevant to build new consumer–resource-type models that combine the approaches proposed in this work and in the paper [43]. Another promising area is designing canopy-level numerical modeling frameworks, e. g., by extending the one tested in [43].

Acknowledgements The authors acknowledge the support of the French Agence Nationale de la Recherche 664 (ANR) under Grant ANR-13-BSV7-0011 (project FunFit).

References

1. Akhmetzhanov AR, Grognard F, Mailleret L, Bernhard P (2012) Join forces or cheat: evolutionary analysis of a consumer-resource system. In: Advances in dynamic games, volume 12 of the series Annals of the International Society of Dynamic Games, Springer, New York, pp 73–95
2. Akhmetzhanov AR, Grognard F, Mailleret L (2011) Optimal life-history strategies in seasonal consumer-resource dynamics. Evolution 65(11):3113–3125
3. Bancal MO, Hansart A, Sache I, Bancal P (2012) Modelling fungal sink competitiveness with grains for assimilates in wheat infected by a biotrophic pathogen. Ann Bot 110(1):113–123
4. Berkovitz LD (1985) The existence of value and saddle point in games of fixed duration. SIAM J Control Optim 23(2):172–196
5. Bernhard P (2014) Pursuit-evasion games and zero-sum two-person differential games. Encycl Syst Control. https://doi.org/10.1007/978-1-4471-5102-9_270-1

6. Bernhard P (1977) Singular surfaces in differential games: an introduction. In: Hagedorn P, Knobloch HW, Olsder GJ (eds) Differential games and applications, volume 3 of the series Lecture Notes in Control and Information Sciences. Springer, Berlin, pp 1–33
7. Bernhard P (1987) Differential games: closed loop. In: Singh MG (ed) Systems & control encyclopedia: Theory, technology, applications. Pergamon Press, Oxford, New York, pp 1004–1009
8. Bernhard P (1987) Differential games: Isaacs equation. In: Singh MG (ed) Systems & control encyclopedia: theory, technology, applications. Pergamon Press, Oxford, New York, pp 1010–1016
9. Bernhard P (2015) Evolutionary dynamics of the handicap principle: an example. Dyn Games Appl 5:214–227
10. Bernhard P, Grognard F, Mailleret L, Akhmetzhanov A (2010) ESS for life-history traits of cooperating consumers facing cheating mutants. [Research Report] RR–7314, INRIA. https://hal.inria.fr/inria-00491489v2
11. Bokanowski O, Desilles A, Zidani H, Zhao J (2017) User's guide for the ROC-HJ solver. May 10. Version 2.3. https://uma.ensta-paristech.fr/soft/ROC-HJ
12. Botkin ND, Hoffmann K-H, Turova VL (2011) Stable numerical schemes for solving Hamilton–Jacobi–Bellman–Isaacs equations. SIAM J Sci Comput 33(2):992–1007
13. Boyle B, Hamelin RC, Séguin A (2005) In vivo monitoring of obligate biotrophic pathogen growth by kinetic PCR. Appl Environ Microbiol 71(3):1546–1552
14. Clarke FH, Ledyaev YuS, Stern RJ, Wolenski PR (1998) Nonsmooth analysis and control theory. Springer, New York
15. Crandall MG, Lions P-L (1984) Two approximations of solutions of Hamilton–Jacobi equations. Math Comput 43:1–19
16. Day T (2001) Parasite transmission modes and the evolution of virulence. Evolution 55:2389–2400
17. Day T (2003) Virulence evolution and the timing of disease life-history events. Trends Ecol Evol 18:113–118
18. Deacon JW (1997) Modern mycology. Blackwell Scientific, Oxford
19. Dercole F, Rinaldi S (2008) Analysis of evolutionary processes: the adaptive dynamics approach and its applications. Princeton University Press, Princeton
20. Dieckmann U, Heino M, Parvinen K (2006) The adaptive dynamics of function-valued traits. J Theor Biol 241:370–389
21. Elliott RJ, Kalton NJ (1972) The existence of value in differential games. Mem Am Math Soc 126:1–67
22. Eshel I, Motro U (1981) Kin selection and strong stability of mutual help. Theor Popul Biol 19:420–433
23. Fleming WH, Soner HM (2006) Controlled Markov processes and viscosity solutions. Springer, New York
24. Friedman A (1971) Differential games. Wiley, New York
25. Geritz SAH, Kisdi É, Meszéna G, Metz JAJ (1998) Evolutionarily singular strategies and the adaptive growth and branching of the evolutionary tree. Evol Ecol 12(1):35–57
26. Gilchrist MA, Sulsky DL, Pringle A (2006) Identifying fitness and optimal life-history strategies for an asexual filamentous fungus. Evolution 60:970–979
27. Hahn M (2000) The rust fungi: cytology, physiology and molecular biology of infection. In: Kronstad JW (ed) Fungal pathology. Springer, Dordrecht
28. Isaacs R (1965) Differential games. Wiley, New York
29. Ivanov GE (1997) Saddle point for differential games with strongly convex-concave integrand. Math Notes 62(5):607–622
30. Krasovskii NN, Subbotin AI (1974) Positional differential games. Nauka, Moscow In Russian
31. Mailleret L, Lemesle V (2009) A note on semi-discrete modelling in life sciences. Philos Trans R Soc Lond A 367:4779–4799
32. Maynard Smith J (1974) The theory of games and the evolution of animal conflicts. J Theor Biol 47:209–221
33. Maynard Smith J, Price GR (1973) The logic of animal conflicts. Nature 246:15–18
34. Melikyan AA (1998) Generalized characteristics of first order PDEs: application in optimal control and differential games. Birkhauser, Boston
35. Metz JAJ (2008) Fitness. In: Jørgensen SE, Fath BD (eds) Encyclopedia of ecology. Academic Press, Oxford, pp 1599–1612
36. Metz JAJ, Stankova K, Johansson J (2016) The canonical equation of adaptive dynamics for life histories: from fitness-returns to selection gradients and Pontryagin's maximum principle. J Math Biol 72:1125–1152
37. Murray JD (2002) Mathematical biology. I. An introduction. Interdisciplinary applied mathematics, volume 17. Springer, Berlin, Heidelberg (2002)
38. Nowak MA (1990) An evolutionary stable strategy may be inaccessible. J Theor Biol 142:237–241

39. Osher S, Shu C-W (1991) High order essentially non-oscillatory schemes for Hamilton–Jacobi equations. SIAM J Numer Anal 28(4):907–922
40. Parthasarathy T, Raghavan TES (1975) Existence of saddle points and Nash equilibrium points for differential games. SIAM J Control 13(5):977–980
41. Parvinen K, Heino M, Dieckmann U (2013) Function-valued adaptive dynamics and optimal control theory. J Math Biol 67:509–533
42. Pontryagin LS, Boltyansky VG, Gamkrelidze RV, Mishchenko EF (1964) The mathematical theory of optimal processes. Macmillan, New York
43. Précigout P-A, Claessen D, Robert C (2017) Crop fertilization impacts epidemics and optimal latent period of biotrophic fungal pathogens. Phytopathology 107:1256–1267
44. Press WH, Teukolsky SA, Vetterling WT, Flannery BP (2007) Numerical recipes: the art of scientific computing. Cambridge University Press, New York
45. Roxin E (1969) Axiomatic approach in differential games. J Optim Theory Appl 3(3):153–163
46. Sasaki A, Iwasa Y (1991) Optimal-growth schedule of pathogens within a host: switching between lytic and latent cycles. Theor Popul Biol 39:201–239
47. Schmitendorf WE (1970) Differential games with open-loop saddle point conditions. IEEE Trans Autom Control 15:320–325
48. Schmitendorf WE (1970) Existence of optimal open-loop strategies for a class of differential games. J Optim Theory Appl 5:363–375
49. Schmitendorf WE (1976) Differential games without pure strategy saddle-point solutions. J Optim Theory Appl 18:81–92
50. Shaiju A, Bernhard P (2009) Evolutionarily robust strategies: two nontrivial examples and a theorem. In: Pourtallier O, Gaitsgory V, Bernhard P (eds) Advances in dynamic games and their applications, vol 10. Annals of the International Society of Dynamic Games. Birkhäuser, Boston
51. Silvani VA, Bidondo LF, Bompadre MJ, Colombo RP, Pérgola M, Bompadre A, Fracchia S, Godeas A (2014) Growth dynamics of geographically different arbuscular mycorrhizal fungal isolates belonging to the 'Rhizophagus clade' under monoxenic conditions. Mycologia 106(5):963–975
52. Subbotin AI (1995) Generalized solutions of first-order PDEs: the dynamical optimization perspective. Birkhauser, Boston
53. Subbotin AI, Chentsov AG (1981) Optimization of guaranteed result in control problems. Nauka, Moscow In Russian
54. Varaiya PP (1967) On the existence for solution to a differential game. SIAM J Control 5(1):153–162
55. Vincent TL, Brown JS (2005) Evolutionary Game Theory, Natural Selection, and Darwinian Dynamics. Cambridge University Press, Cambridge
56. Yegorov I, Grognard F, Mailleret L, Halkett F (2017) Optimal resource allocation for biotrophic plant pathogens. IFAC-PapersOnline 50(1):3154–3159
57. Yong J (2015) Differential games: a concise introduction. World Scientific, Singapore